

ARTICLE



<https://doi.org/10.1038/s41467-022-30833-3>

OPEN

Mitigation of SARS-CoV-2 transmission at a large public university

In Fall 2020, universities saw extensive transmission of SARS-CoV-2 among their populations, threatening health of the university and surrounding communities, and viability of in-person instruction. Here we report a case study at the University of Illinois at Urbana-Champaign, where a multimodal “SHIELD: Target, Test, and Tell” program, with other non-pharmaceutical interventions, was employed to keep classrooms and laboratories open. The program included epidemiological modeling and surveillance, fast/frequent testing using a novel low-cost and scalable saliva-based RT-qPCR assay for SARS-CoV-2 that bypasses RNA extraction, called covidSHIELD, and digital tools for communication and compliance. In Fall 2020, we performed >1,000,000 covidSHIELD tests, positivity rates remained low, we had zero COVID-19-related hospitalizations or deaths amongst our university community, and mortality in the surrounding Champaign County was reduced more than 4-fold relative to expected. This case study shows that fast/frequent testing and other interventions mitigated transmission of SARS-CoV-2 at a large public university.

A full list of authors and their affiliations appears at the end of the paper.

It has been very challenging to control the spread of SARS-CoV-2 worldwide. Strategic deployment of non-pharmaceutical interventions has relied primarily on combining laboratory performance characteristics with theoretical modeling to estimate real-world outcomes. However, this proved particularly challenging during Spring and early Summer 2020 due to limited availability of data on viral load dynamics through different disease stages especially the pre-symptomatic shedding phase, the lack of consensus on the dominant mode of transmission of COVID-19 specifically the controversy about the role of airborne route¹, and the lack of a quantitative framework for the interplay between human behavior and transmission dynamics^{2,3}. Colleges and universities have proven to be especially difficult environments. As our ~35,000 undergraduate students at the University of Illinois at Urbana-Champaign (UIUC) departed campus to continue their education remotely in Spring of 2020, we recognized their return in the Fall would present significant challenges. Our biggest concern was that unmitigated transmission amongst our undergraduate student population would drive increased cases in our faculty and staff and/or the surrounding Champaign County community. In fact, many universities saw extensive transmission of SARS-CoV-2 among their populations in the Fall of 2020, threatening the health of students, faculty and staff, the viability of in-person instruction, and the health of surrounding communities^{4,5}.

Here, we show that population scale-deployment of a multimodal platform of non-pharmaceutical interventions, centered on fast/frequent testing with a novel saliva-based RT-qPCR assay for SARS-CoV-2 that bypasses RNA extraction, called covidSHIELD, effectively mitigated transmission of SARS-CoV-2 at a large public university and its surrounding community. The SHIELD: Target, Test, and Tell program was devised to mitigate SARS-CoV-2 transmission through identification and isolation of infected individuals before they spread the virus. This program worked in concert with other non-pharmaceutical interventions, including masks, social distancing, and robust education efforts, to allow us to achieve our transmission mitigation goal.

Since the tools needed to implement this 3-part strategy were not available at the time, they were each created during the Summer of 2020. This was a time of great uncertainty as the future trajectory of the pandemic was unknown and many campuses had doubts about budget and finances during the following academic year⁶. Several studies started to surface as early as June 2020 about feasibility of college reopening in the fall 2020^{7–11}. However, conclusions varied widely from suggesting that there is no way to reopen universities safely¹² to suggesting that bringing students back to class will make them safer¹³. There was a need for developing a tailored model for safe reopening of a large public university, like the University of Illinois, located in a college town, having a vibrant residential student program, and with the university population constituting almost 25% of the town population.

Results

Target. For the *Target* component of the SHIELD program, epidemiological modeling helped determine how often the university population should be tested, and real-time data analysis further allowed for strategic adjustments to testing schedules throughout the semester to maximally mitigate spread. We note that all epidemiological modeling requires assumptions, which means that the predictive capacity of such modeling always has limitations. For a detailed description of the methods employed and assumptions included in our modeling studies, please see Methods section.

Given early data suggesting that SARS-CoV-2 can be transmitted by pre-symptomatic and asymptomatic carriers^{14–19}, fast and frequent testing of all individuals in the university community was expected to be critical for mitigating localized outbreaks by enabling identification and isolation of infected individuals prior to clinically impactful shedding of SARS-CoV-2^{20,21}. Available data on viral dynamics^{19,20,22,23} suggested that test results should be returned within hours, not days, and that testing might need to be performed multiple times per week, particularly for the populations most likely to be exposed to SARS-CoV-2. To explore these issues quantitatively, we used a variety of methods to arrive at an optimal strategy for our campus.

We calculated how the basic reproduction number, R_0 , is modified by a multiplier, M , that accounts for the fact that if an individual is detected to be positive and immediately isolated, they are unable to continue infecting others. This results in a fractional reduction of R_0 ($R_t = M R_0$) as detailed in Fig. 1a. Using an infectivity profile that includes pre-symptomatic shedding^{19,24}, we could calculate M as a function of testing frequency (see the “Methods” section). We found that testing everyone every 7 days yields $M = 0.71$, but testing everyone every 3.5 days yields $M = 0.45$, because their infectious period while not isolated (Area A in Fig. 1a) is reduced. These estimates are conservative as we neglected the intrinsic reduction in transmission for truly asymptomatic individuals compared to symptomatic individuals (e.g., Kissler et al., 2021²⁵) This simplification is justified as the goal was to control the epidemic in the worst-case scenario.

We also simulated the spread of COVID-19 on campus using agent-based modeling, following each student as they attend university activities and participate in off-campus socializing (see the “Methods” section for key assumptions and details, which included early recognition that SARS-CoV-2 is spread via airborne transmission²⁶). As shown in Fig. 1b, this analysis predicted that masking or the combination of masking and social distancing would provide inadequate protection against spreading of COVID-19 ($R_0 > 1$). However, the addition of twice per week testing was predicted to make R_0 manageable ($R_0 < 1$). The additional inclusion of testing-enabled manual contact tracing and digital exposure notifications predicted even further reductions. In fact, the model predicted these mitigation approaches would be synergistic and highly effective when applied in concert, with R_0 small enough to contain the epidemic when using the full suite of twice-weekly testing of everyone on campus, isolation of newly infected people, contact tracing, quarantining and use of the Safer Illinois exposure-notification app, along with masking and social distancing. These general trends were robust within the validated boundary conditions of the underlying assumptions (see the “Methods” section and Supplementary Fig. 1). These simulations reinforced that the effectiveness of testing, isolation and contact tracing in reducing transmission was heavily dependent on rapid turnaround, because of the high transmissibility of COVID-19, in agreement with other modeling results²⁷.

Test. When considering various testing options, the evaluation of virus levels in saliva was highly attractive due to the known detection of SARS-CoV-2 through oral shedding and the potential for rapid, easy, and non-invasive self-collection^{28–30}, thus minimizing the need for direct healthcare provider–patient contact and consequent conservation of personal protective equipment (PPE). Numerous reports have detailed the detection of SARS-CoV-2 in saliva^{31–35}, and salivary/respiratory aerosols and droplets are recognized as a significant factor in person-to-person transmission of SARS-CoV-2²⁸. However, all saliva-based assays available in the Spring of 2020 required RNA isolation, which added cost, time, and supply chain bottlenecks.

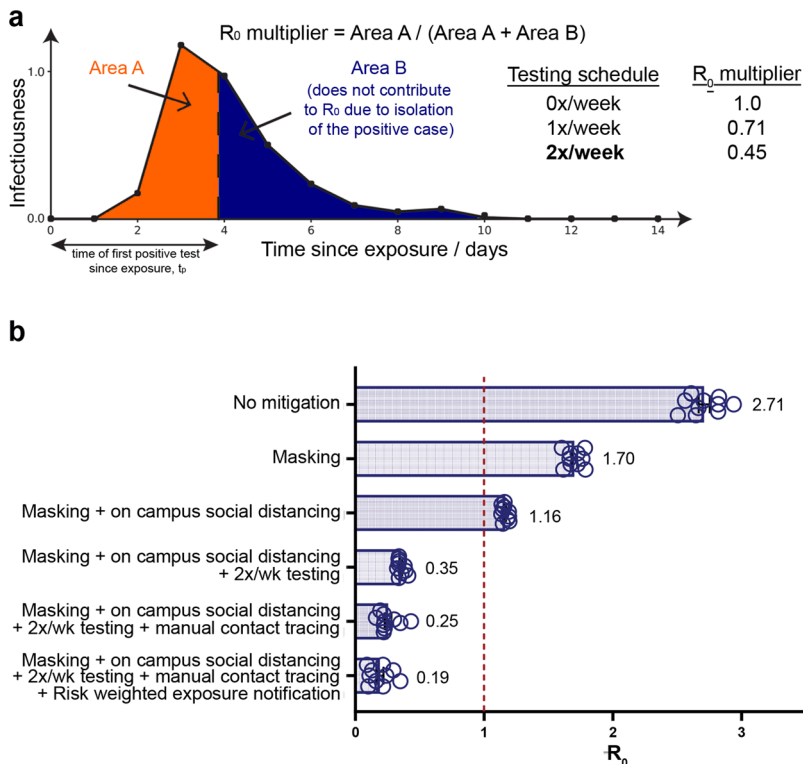


Fig. 1 Target. **a** Sensitive testing can reveal a positive case early in the infection, and thus isolation of the index case reduces the number of people infected by this index case. Frequent testing and rapid isolation reduce the time period during which a person is infectious but not isolated (Area A). As a result, the R_0 multiplier for testing is the ratio between the truncated area under the curve (Area A) and the untruncated area under the curve (Area A + Area B). The dashed vertical line between Area A and Area B represents the moment an infected individual is isolated; as this line moves to the left, M is decreased and viral spread is reduced. **b** Effect of different mitigation interventions on the basic reproduction number R_0 as computed in our agent-based model. Mean R_0 values ($n = 10$) are indicated for each conditions tested. Error bars represent SEM. If R_0 is >1 (orange dashed line at $R_0 = 1$), the epidemic grows exponentially. If R_0 is <1 , any outbreak diminishes exponentially. Without any mitigation, R_0 is close to 3 and a runaway epidemic will occur. Masking and social distancing help reduce transmission but can't suppress growth of cases on their own as R_0 is still greater than one. However, when these measures are combined with frequent testing (2 tests a week), R_0 drops to 0.35 and containment of epidemic becomes possible. Adding extra mitigation interventions such as manual contact tracing and risk based exposure notification being R_0 further down to 0.19 suggesting the potential for strong control of the epidemic on campus. The details of the agent-based model are given in the "Methods" section. The results shown here are computed assuming that 100% of the students are compliant with twice a week testing, isolation, and quarantine. We also ran the same simulation assuming 60% compliance, and the same general trends were observed with R_0 for the full SHIELD program predicted to still be manageable (0.5, see Supplementary Fig. 1). Simulated effects of delays and imperfect contact tracing on the final size of epidemic and peak quarantined population, using the agent-based model, are shown in Supplementary Fig. 2.

With the goal of performing up to 20,000 individual RT-qPCR tests for SARS-CoV-2 per day, we developed a saliva-based assay for SARS-CoV-2 nucleic acid detection that bypasses RNA isolation/purification³⁶ (called covidSHIELD). This process relies on up-front heating of freshly collected saliva samples, an attractive and simple method to inactivate the virus without having to open the collection vessel. Using intact, γ -irradiated SARS-CoV-2 spiked into fresh human saliva (that was confirmed to be SARS-CoV-2 negative), we observed substantial time- and temperature-dependent improvement in SARS-CoV-2 nucleic acid detection by direct RT-qPCR, without the use of RNA extraction (Fig. 2a). When incubated at ambient temperature (no heat treatment), no SARS-CoV-2 genes are detectable, but as temperature and incubation time increase, substantial improvement in viral nucleic acid detection is observed, with 100% identification of the three targeted SARS-CoV-2 genes, in all replicate samples, detected following a 30 min incubation at 95 °C. Importantly, a short heating time (5 min) at 95 °C (as has been examined by others^{37,38}) does not allow for sensitive detection; the 30-min duration is essential, as it is likely that this extended heating drives temperature-dependent inactivation of components of saliva that inhibit RT-qPCR. Preliminary

comparison of this heating-based RNA extraction-free protocol to a standard protocol involving RNA isolation using 25 split clinical saliva samples showed 100% concordance between the two assays (Fig. 2b and Supplementary Table 1), suggesting that the heat-inactivation step does not affect assay outcome. This RNA extraction-free protocol, which is based upon the detection of three viral genes—replicase polyprotein 1ab (*ORF1ab*), nucleocapsid (*N*-gene), and spike protein (*S*-gene) using the TaqPath COVID-19 Combo kit is also highly sensitive (limit of detection of 500–1000 SARS-CoV-2 viral copies/mL, Supplementary Fig. 3), can be optimized for high-throughput using robotic sample transfers with no impact on sensitivity (Supplementary Table 2), is minimally affected by exogenous and endogenous potentially interfering substances (Supplementary Table 3), yields stable results for up to 7 days when the saliva is stored below 25 °C prior to heat inactivation (Supplementary Fig. 4), and is also compatible with other RT-qPCR primers (such as the CDC primers targeting *N* gene, Supplementary Fig. 5). Head-to-head comparison with a subsequently developed direct saliva to RT-qPCR technique that requires opening of tubes and addition of proteinase-K to saliva samples prior to heat inactivation³⁹ shows that the simple covidSHIELD protocol for viral inactivation

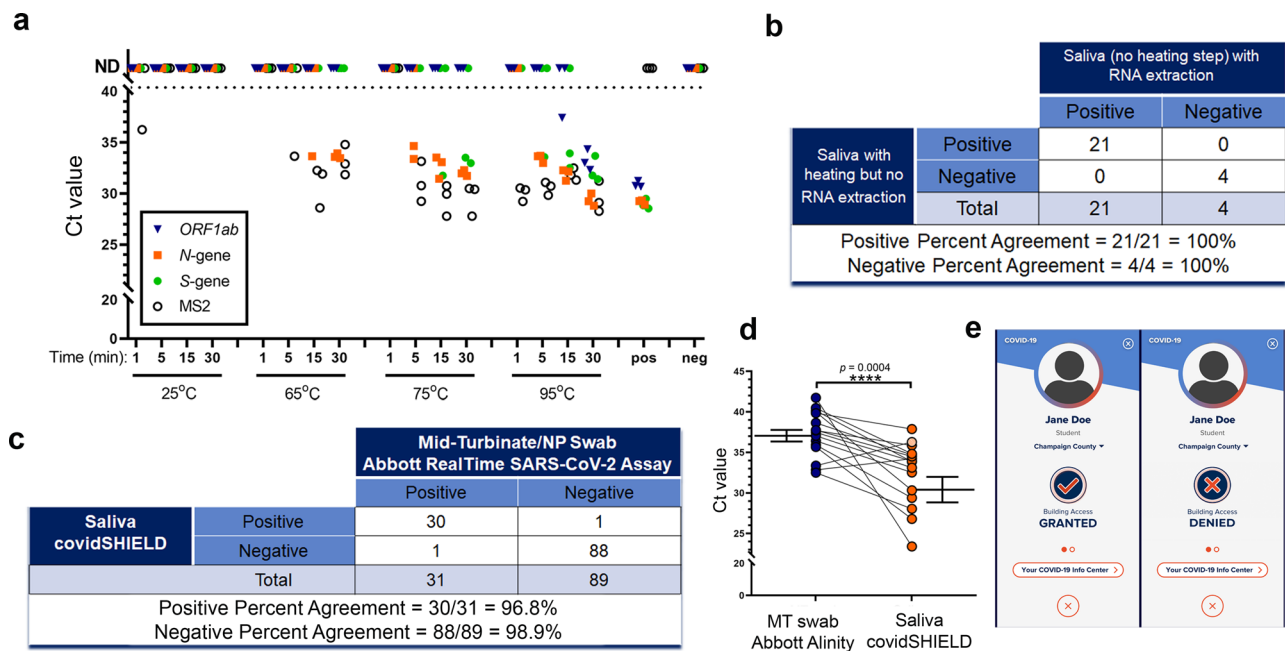


Fig. 2 Test and tell. **a** The effect of heat on SARS-CoV-2 nucleic acid detection in saliva. γ -irradiated SARS-CoV-2 (1.0×10^4 viral copies/mL) was spiked into fresh human saliva (SARS-CoV-2 negative). Samples diluted 1:1 with $2\times$ Tris-borate-EDTA (TBE) buffer were incubated at 25 °C, or in a hot water bath at the indicated temperature and incubation time. All saliva samples were spiked with purified MS2 bacteriophage as an internal control and directly analyzed by RT-qPCR, in triplicate, for SARS-CoV-2 nucleic acid corresponding with *ORF1ab* gene, *N*-gene, and *S*-gene. Undetermined Ct values are plotted as ND. This experiment was repeated at least three times. **b** 25 clinical saliva samples were split into two aliquots upon receipt, one set was processed using our covidSHIELD assay and the other set was subjected to RNA extraction. 5 μ L of processed saliva were subsequently used as templates for RT-qPCR. A positive result is called when two out of three viral target genes is detected. **c** Qualitative outcome of parallel testing of paired mid-turbinate swabs and saliva with the Abbott RealTime SARS-CoV-2 assay and covidSHIELD. 120 participants were enrolled in a clinical study comparing results from contemporaneously collected nasopharyngeal or mid-turbinate nasal swabs analyzed using both protocols. Overall concordance was 98.3% (95% CI, 94.1–99.8%), positive percent agreement was 96.8% (95% CI, 83.2–99.9%) and negative percent agreement was 98.9% (95% CI, 93.9–99.9%). All clinical trials were reviewed by the Western Institutional Review Board. All participants gave written and informed consent. **d** Additional clinical study outcome of 17 individuals confirmed to be positive for COVID-19 and to have low viral loads (Ct = 32–42, average 37) by mid-turbinate nasal swabs analyzed at the Johns Hopkins University School of Medicine using Abbott Alinity compared with contemporaneously collected saliva samples that were analyzed using the covidSHIELD assay at the University of Illinois Urbana-Champaign CLIA-registered laboratory. p -value = 0.0004 was calculated using 2-tailed, unpaired t -test. **e** Mock representative images from the Safer Illinois app. The screen on the left appears when a user is in compliance with the campus testing protocol and has received a recent negative test for SARS-CoV-2. The screen on the right appears when the user of the app is out of compliance, when they have had a recent exposure notification, or when they have tested positive for the virus.

results in approximately 8-fold more sensitive detection using the TaqPath COVID-19 Combo kit (Supplementary Fig. 6).

In parallel to the work on test development, we created a dedicated CLIA-registered laboratory in our on-campus Veterinary Diagnostic Laboratory that includes semi-robotic capacity to efficiently process up to 20,000 saliva samples per day. We also set up \sim 20 saliva collection stations throughout campus and all associated infrastructure for hourly delivery of samples to the CLIA lab.

A clinical study was performed with 120 individuals suspected of COVID-19 by their healthcare provider to compare the results of the covidSHIELD assay to results from contemporaneously collected nasopharyngeal or mid-turbinate nasal swabs analyzed by an FDA Emergency Use Authorized reference method for detection of SARS-CoV-2. Samples were collected at four different geographically distinct sites (one in Urbana, IL; one in Madison, WI; two in Chicago, IL). All nasal swab samples were analyzed in the clinical pathology laboratory at the University of Illinois Chicago Hospital using the Abbott RealTime SARS-CoV-2 assay performed on the Abbott m2000 System with a LoD of 2700 NDU/mL, and all saliva samples were analyzed using the covidSHIELD assay at the University of Illinois Urbana-Champaign CLIA-registered laboratory. Participants were all over the age of 18 and suspected to have COVID-19 (either with

symptoms or with known exposures to someone positive for COVID-19). Of the 120 sample sets that were collected, 31 of the nasal samples were found to be positive and 89 of the nasal samples were found to be negative (Fig. 2c, Supplementary Table 4). Excellent overall concordance (98.3%, 95% CI, 94.1–99.8%), positive percent agreement (96.8%, 95% CI, 83.2–99.9%) and negative percent agreement (98.9%, 95% CI, 93.9–99.9%) were observed for the covidSHIELD assay on the contemporaneously collected saliva samples (for more detailed information on the clinical study, see the “Methods” section and Supplementary Tables 5, 6).

An additional clinical study was performed with 17 individuals confirmed by mid-turbinate nasal swabs analyzed at the Johns Hopkins University School of Medicine to be positive for COVID-19 and to have low viral loads (Ct = 32–42, avg. 37). Contemporaneously collected saliva samples were then analyzed using the covidSHIELD assay at the University of Illinois Urbana-Champaign CLIA-registered laboratory. As shown in Fig. 2d, the covidSHIELD assay detected at least two genes for SARS-CoV-2 in 16/17 of these low viral load samples, and one gene for SARS-CoV-2 was detected in the 17th sample. In 15 out of these 17 samples, the average Ct values for the covidSHIELD assay were lower than that of their matched nasal swabs, and the overall average Ct value for the covidSHIELD assay was significantly

lower than that of nasal swab-based test (Avg Ct for covidSHIELD = 31.82, average Ct for nasal swabs = 37.05, $p < 0.0004$) (For more detailed information on the clinical study, see the “Methods” section and Supplementary Table 7). More recent studies have further demonstrated that covidSHIELD is highly effective for detecting infected individuals early in the disease, and throughout the period of infectiousness, that viral genome loads tend to peak earlier in the covidSHIELD saliva-based RTqPCR assay relative to a standard nasal swab-based RTqPCR assay⁴⁰.

The U.S. Food and Drug Administration has granted Emergency Use Authorization to the covidSHIELD test: EUA202555 SUMMARY covidSHIELD Assay (<https://www.fda.gov/media/146317/download>).

Tell. It was critical to maximize the speed and effectiveness with which the results of the covidSHIELD assay could be communicated, and to couple these results to participation in desired activities to encourage compliance. To achieve these goals, a multidisciplinary team developed a COVID-19 app called Safer Illinois. The app automatically receives the results of the SARS-CoV-2 tests performed at the UIUC CLIA-registered Lab in a manner that is privacy-preserving and HIPAA compliant. The app also displays a cover screen that grants or denies access to campus buildings based on an individual’s most recent covidSHIELD test results (Fig. 2e). A proximity-based and thus privacy-preserving exposure notification feature warns users when they have been in significant contact with someone who has recently tested positive. In order to maintain “Building Access Granted” status, an individual must be up to date on their required testing frequency, not have recently tested positive for COVID-19, and not have a recent exposure notification from the app. The Building Access feature is a key driver of compliance with the testing protocol. The code for Safer Illinois was made publicly available and independently audited by three different independent expert groups. Survey results and online town hall style meetings showed that in general the privacy-preserving features of the app were well-appreciated, but there were still some concerns about privacy and potential for data sharing. Thus, we decided not to mandate the use of Safer Illinois. People could alternatively choose to receive their covidSHIELD test results via a secure email through the campus’ McKinley Health Center, and/or utilize a web-based process to communicate their building entry status.

Deployment during Fall 2020. After an encouraging pilot study in July 2020, we deployed the complete SHIELD: Target, Test, and Tell platform, in concert with other non-pharmaceutical interventions including masks, social distancing, and robust education efforts, across our entire community of undergraduate and graduate students, postdoctoral associates, staff and faculty, a population of about 50,000 people, from the time our undergraduates returned on August 15, 2020 until the last scheduled day of the semester on December 23, 2020. Participation in the SHIELD program was required for all students living in Champaign-Urbana, and for all faculty and staff that chose to access campus buildings. From matching testing records with enrollment data we estimate that ~60% of our students were highly compliant with the required testing throughout the semester, most of the remainder were somewhat compliant, and there was a minority of students who were non-compliant. These estimates were also consistent with the observed probability distribution function for the time interval between tests for the student population which suggested that the mean time between tests was 4.4 days, the probability of inter-test time larger than 7 days is

11%, and that 62% of the tests were spaced at 3.5 days or less (see Supplementary Fig. 7). As summarized in Fig. 3a, during this time we performed >1,000,000 covidSHIELD tests with an average turnaround time of 11.2 h, and we kept classrooms, research laboratories, and many other University activities open. There were more than 49,000 unique users of Safer Illinois (approximately 94% of the individuals who were eligible to be tested). Over the semester, 94% of the virus test results were transmitted via the app. There were 3.95 million Safer Illinois app sessions (IOS users, 77%; Android users, 23%), more than 920,000 views of the Building Entry Status, 166,000 views of Testing Locations, 26,600 views of Health Guidelines, 25,000 views of the Health Care Team page, and 1160 digital exposure notifications. During this time period, our new daily COVID-19 case positivity rates were less than 0.5% for 75% of the days, we had no evidence of spread within our classrooms or research laboratories based on contact tracing information per case investigations conducted by Champaign Urbana Public Health Department (CUPHD), and we also had zero COVID-19-related hospitalizations or deaths among our campus community.

Although in general our positivity rates remained low, there were four periods during the Fall semester during which we observed transient increases in the number of daily cases (Periods I–IV indicated in Fig. 3a). The most notable example occurred at the beginning of our semester (Period I). Based on our modeling we expected that several hundred of our ~35,000 undergraduate students would be infected with SARS-CoV-2 when they returned to our campus in mid-August 2020 (see the “Methods” section). The university required students to test as soon as they arrived on campus, and they were not permitted access to any campus buildings until they received a negative test result. From August 12 to 23, we conducted a total of 55,034 tests and detected 288 new cases of COVID-19, yielding a new case-positivity rate of 0.52%. During the period of August 24–September 21, our covidSHIELD testing revealed a spike in cases (Fig. 3a). Because we were testing everyone in our community twice per week, we had an early warning signal and comprehensive dataset that allowed us to respond in a data-driven manner. More than 95% of the new positive cases were in undergraduates, and we identified several clusters in buildings where social activities inconsistent with campus recommendations had been reported. Contact tracing combined with covidSHIELD testing data revealed early signs of potential outbreaks in these buildings.

Guided by these data, we did three things: First, we required that all undergraduate students engage only in essential activities for 2 weeks. Essential activities were defined as in-person classes, laboratory activities, employment responsibilities, solo outdoor exercise, religious activities and grocery shopping. Second, we modified our testing protocols to prioritize fast and frequent testing of undergraduates, especially those at highest risk of transmitting COVID-19. Undergraduates living in buildings with high numbers of positive cases were required to test three times per week, all other undergraduates continued to be required to test twice per week, and all faculty, staff and graduate students were switched to once per week. Third, we increased the speed with which undergraduates who tested positive were isolated using text messaging. While we cannot determine the specific impact of these interventions, our observation was that over the course of the next two weeks, our daily case positivity rate dropped from a peak of 2.86% on August 30 to 0.25% on September 12 (Fig. 3a). Furthermore, we conducted a retrospective analysis in mid-October 2020, using our agent-based model, to explore the impact of compliance with isolation and quarantine, imported infections from surrounding community, as well as the essential activities period on the trajectory of cases (Supplementary Fig. 8). The results reinforced the critical role of compliance in shaping the epidemic curve and suggested that

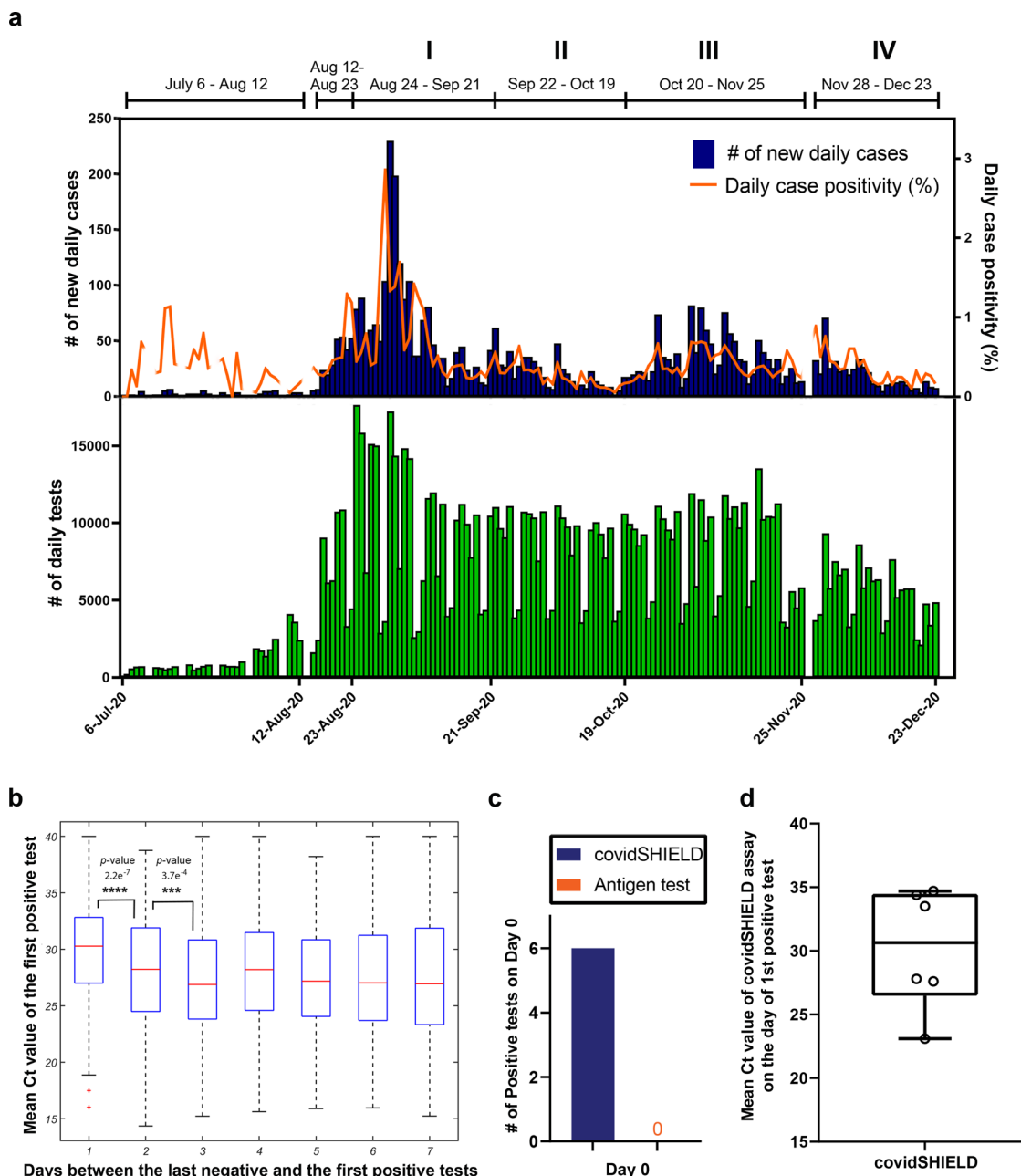


Fig. 3 Deployment of frequent repeat testing at the University of Illinois in fall 2020. **a** Timeline of detected cases during surveillance testing from July 6 to December 23, 2020. The top panel displays the daily new cases (blue) and the daily case positivity (orange). The daily case positivity is computed as the (number of new cases)/(unique number of individuals tested during the day). The lower panel shows the number of daily tests performed (green), which to an excellent approximation is the same as the number of unique individuals tested in a day. **b** Ct values of the first positive test as a function of time elapsed since the last negative test. The difference between the first (1 day) and the second (2 days) bins is highly statistically significant (p -value $2.2e^{-7}$), and that between the second (2 days) and the third (3 days) bins is statistically significant (p -value $3.7e^{-4}$). p -values shown are for the two-sided hypothesis of non-zero Pearson correlation between the number of days since the last negative test (x -axis) and the Ct value of the first positive test (y -axis). The exact sample sizes are: 341 patients who test positive 1 day since the last negative, 616 patients—2 days since the last negative, 716 patients—3 days since the last negative, and 1230 patients—between 4 and 7 days since the last negative. The box plots were generated using the command boxplot in Matlab 9.10.0.1684407(R2021a). The bottom and top of each box are the 25th and 75th percentiles of the sample, respectively. The distance between the bottom and top of each box is the interquartile range. The red line in the middle of each box is the median. The whiskers go from the end of the interquartile range to the furthest observation within the whisker length which is $1.5\times$ the interquartile range. The outliers are marked with red + sign and are defined as the observations that go beyond the whisker length. **c** Head-to-head daily testing with covidSHIELD and antigen-based lateral flow assays in a subgroup of participants ($n = 190$) from October 1, 2020 to Dec 23, 2020. A total of 13,299 contemporaneous tests were performed. Of the 190 individuals, 6 tested positive for SARS-CoV-2 on Day 0 using the covidSHIELD test but all six tested negative using the antigen test. Blue and orange bars represent the percentage of participants that tested positive for SARS-CoV-2 on day 0 using covidSHIELD and the antigen test, respectively. **d** Box-and-whiskers plot of mean Ct values of the 6 individuals who tested positive for SARS-CoV-2 using the covidSHIELD assay on Day 0. Data was plotted using GraphPad Prism v9.3.1, where the lower and upper box extends from 25th to 75th percentiles, respectively, the line in the middle of the box is the median, the lower and upper error lines are the minimum and maximum value, respectively; each individual values are plotted as circles superimposed on the graph.

higher compliance levels and reduced social activities during the essential activities period were successful in quickly containing the initial spike. Comparing the observed case count and the model trajectories suggested that compliance levels varied over time, was highest during the temporary restrictions period, and was generally between 50% and 70% depending on the number of daily imported infections. The latter is an important confounder to consider especially during periods of high community transmission.

For the remainder of the semester, we continued to perform the same approach focused on risk-prioritized fast/frequent testing and rapid isolation. All three of the subsequent increases in cases were similarly followed by rapid declines (Periods II–IV). Period IV is also notable. Classes were pre-scheduled to be moved online after Thanksgiving break, but student surveys revealed that 60% of undergraduates planned to return to Champaign-Urbana after the Thanksgiving break. We expected an increase in cases stemming from travel and holiday gatherings, and we were concerned about social activities during the cold month of December. Thus, all undergraduate students that chose to return to Champaign-Urbana were required to test three times per week. During this time, we also returned faculty, staff and graduate students to a twice-per-week schedule. After a small spike upon the students' return, our case positivity quickly reduced and generally remained low, reaching 0.25% as we passed the 1,000,000 test mark on December 15. We ended the semester on December 23 with a case positivity rate of 0.16%.

Analysis of viral load. Because we were testing people in our campus community once, twice, or three times per week, by the time we reached September 2 we had documented negative tests for most of our campus community. This indicated that people testing as new positives were generally still in the early stages of infection. Prior studies suggest that Ct values of >25 (corresponding to lower viral loads) are correlated with reduced ability to recover infectious virus and hence individuals with Ct > 25 pose a lower risk for transmission^{21,41–45}. For the people that first tested positive with the covidSHIELD assay from September 2 to December 23, 73% had recorded Ct values that averaged >25, and the average Ct value was even higher when the most recent negative test occurred within the past few days (Fig. 3b). The covidSHIELD assay was thus likely detecting many of these new positive cases prior to infectiousness.

Head-to-head daily testing with covidSHIELD and an antigen-based lateral flow assay. We also compared the covidSHIELD assay to a lateral flow assay/antigen test for COVID-19. Specifically, a subset of participants in the Division of Intercollegiate Athletics ($n = 190$) were tested every day with both the covidSHIELD saliva RT-qPCR assay and the Quidel Sofia 2 SARS-CoV-2 MT swab Antigen FIA assay from October 1, 2020 to December 23, 2020, for a total of 13,299 contemporaneous tests. This real world daily testing of asymptomatic people enabled comparison of these two testing methods for their ability to identify infected individuals and remove them from the population in the early stages of infection. As shown in Fig. 3c, this study found six SARS-CoV-2 positive participants during the entire period. All six were identified as positive via the covidSHIELD assay and confirmed to be positive by a subsequent positive covidSHIELD test within the following 4 days. None of these individuals tested positive on the contemporaneously performed lateral flow assays (Fig. 3c). The initial average Ct value for the covidSHIELD test in these six individuals was 30.2 ± 4.73 (Fig. 3d), consistent with the findings in Fig. 3b. We note that while the results of this focused study are consistent with the

greater sensitivity of the covidSHIELD assay, they do not allow us to make any conclusions as to whether such greater sensitivity would make a difference to epidemic control. We include them here as important comparator data for the diagnostic approach.

Analysis of mitigation of SARS-CoV-2 transmission. To probe the extent to which SHIELD reduced transmission on campus, we estimated the time-dependent reproduction number (R_t) and growth rate throughout the whole semester, highlighting four time periods (I–IV) during which we had observed transient increases in cases of COVID-19 (Fig. 4). The case numbers fell exponentially in time following each of these episodes. The calculations were done using the package EpiNow2⁴⁶ which implements several open-source tools⁴⁶, and current best practices⁴⁷. The cases by date of infection were estimated based on a stochastic distribution of delays guided by the distribution of interval between consecutive tests (Supplementary Fig. 7). Additional details are provided in the “Methods” section. Generally, these estimates demonstrate that R_t reached as low as 0.5, and was frequently around 0.75–0.85. These values are also broadly consistent with those inferred using the formulation outlined in⁴⁸ ($R_t \sim 0.55$ – 0.78) based on the estimated piece-wise constant exponential decay rate of cases during each period of containment (see Supplementary Fig. 9).

We also sought to quantitatively assess the extent to which cases within the campus community influenced or were influenced by each other, and/or by cases in the surrounding community, by examining correlations between sub-populations of the university and surrounding communities. Such an analysis can only reveal the average trends and correlations, and cannot rule out specific instances of transmission that do not conform to the trends. As shown in Fig. 5a, the number of 7-day averaged daily new cases of faculty/staff strongly correlated with that of residents in Champaign County, especially after October 18 (Pearson correlation coefficient 0.86, p -value 7.99×10^{-38} , Supplementary Fig. 10a). At the beginning of the semester (around August 31) when there was a short duration spike in daily new cases from undergraduate students, it had little influence on the faculty/staff (Fig. 5b) or on the surrounding Champaign County community (Fig. 5c). Later in the semester (after October 18), as the number of positive cases in Champaign county and faculty/staff increased, the number of cases of undergraduate students followed similar trends (Fig. 5b, c; Pearson correlation coefficient for number of cases between undergraduates and faculty/staff = 0.88, p -value 1.33×10^{-21} , Supplementary Fig. 10b). All of these data, and additional data from time correlations of residents of Champaign County, undergraduates and faculty/staff (Supplementary Fig. 10) indicate that both faculty/staff and Champaign County cases were essentially uncorrelated with the undergraduate students. Thus the campus population did not drive cases within the surrounding community.

Other communities with or without SHIELD. To further evaluate the efficacy of the SHIELD program, we compared our results to those observed by other communities operating with or without fast/frequent testing with the covidSHIELD assay but which may have been implementing other non-pharmaceutical interventions such as masking and social distancing, as well as symptomatic testing.

We first looked at other communities that started using SHIELD sometime in the Winter or Spring of 2020/2021. As shown in Fig. 6a, another university initiated the use of SHIELD at the beginning of the Spring semester in mid-January 2021. The observed initial 7-day average positivity rate for this community

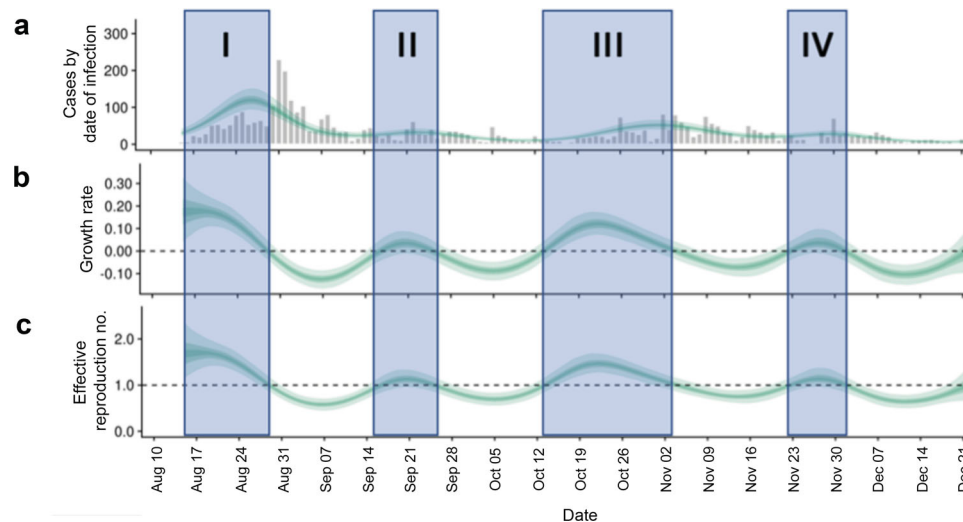


Fig. 4 Epidemiological analysis for COVID-19 cases on campus. **a** Cases estimated by date of infection. **b** Estimated growth rate. **c** Estimated effective reproduction number R_{eff} by the date of infection as a function of time using the method of Cori et al. assuming gamma-distributed generation time distribution⁶² and a distribution between consecutive tests shown in Supplementary Fig. 7. The shaded periods (I–IV) correspond to periods of the semester when $R_{\text{eff}} > 1$ suggesting transient growth of cases. The unshaded time periods correspond to $R_{\text{eff}} < 1$ suggesting that the epidemic is controlled, and cases are decreasing. In each subplot, the credible intervals for the calculation of that output are shown with three shades. These three shades correspond to credible intervals of 20% (darkest green), 50% (lighter green), and 90% (lightest green). Analysis was done using Epidemiological toolbox EpiNow2⁴⁶. Please see the “Methods” section for more details.

was $>0.7\%$. This was rapidly reduced over the period of one month after the introduction of SHIELD, and the positivity rate reached $<0.1\%$ by the end of the Spring 2021 semester.

SHIELD testing was similarly introduced in the middle of the Spring semester at a pair of high schools that required masking and social distancing for the entire semester (Fig. 6b). The observed 7-day average positivity rate was initially found to be $\sim 0.5\%$, and after the introduction of SHIELD, this was quickly reduced to and maintained for the rest of the semester at $\leq 0.1\%$. This provided an opportunity to observe the positivity rate before and after the impact of SHIELD. Similar results were observed at a federal courthouse and a large corporate campus, and again masking and social distancing were in place before and after the introduction of SHIELD (Fig. 6c, d).

Finally, we compared predicted and observed COVID-19 cases and mortality among all U.S. counties with large university enrollments (large enrollment $>15,000$ enrolled students at start of Fall 2020 semester, $n = 251$) from July 6 to December 23, 2020. To account for delays between COVID-19 exposure and outcome (e.g., recovery or death), a 3-week lag was integrated⁴⁹. This allowed us to compare the outcomes for UIUC’s surrounding Champaign County to those of the other similarly sized American Universities, most of which had similar requirements for masking and social distancing, but none of which had the SHIELD program. To account for the potential effects of socio-economic disparities and the demographic makeup of a given county, the overall mean COVID-19 case and mortality rate in each county was age-adjusted and assessed as a function of social vulnerability using linear regression (Fig. 7a). The social vulnerability index is used as a proxy to determine a community’s ability to prevent human suffering and financial hardships in the event of a disaster⁵⁰. We also controlled our analysis by state, given the widely varying policy factors that influence mortality rates (e.g., mask mandates, business closings, etc.). Using a best-fit model for all large university counties, Champaign observed statistically significantly lower COVID-19 cases than predicted (32.5%

reduction in cases, 95% CI: 31.1–33.9; Fig. 7a). More importantly, Champaign County was the county with the greatest reduction in deaths, reducing mortality more than 4.3-fold over expected (95% CI 3.3–5.5; Fig. 7b). The population of Champaign County is $\sim 210,000$ and the testing population in the SHIELD program is $\sim 52,000$. Although a fraction of individuals in the testing population do live outside Champaign County, it is reasonable to estimate that 25% of the county’s population is involved in the SHIELD program. This analysis provides strong evidence that the SHIELD Target, Test, and Tell program uniquely resulted in a protective effect for the communities in Champaign County compared to other communities which may have implemented some non-pharmaceutical interventions or symptomatic testing but did not use the high-frequency surveillance testing combined with real-time analysis of test results and potential exposures.

Discussion

In this case study, scaled deployment of the multimodal “SHIELD: Target, Test, and Tell” platform, in concert with other non-pharmaceutical interventions, mitigated the spread of COVID-19 at a large public university and allowed for the continuation of in-person classes amidst the pandemic. Even though our classes, laboratories and local businesses stayed open, we found no evidence of transmission from students to faculty or staff, no evidence of transmission from the university community to the surrounding community, and no one in our campus community became seriously ill or died as a result of COVID-19 during this timeframe.

We note that because all of these mitigation methods were deployed in parallel and there were no internal control studies, there are limitations regarding attribution of these favorable outcomes to specific interventions. In concert with the SHIELD: Target, Test, and Tell program other non-pharmaceutical interventions such as masking, social distancing, and robust education efforts are likely to have also made a significant impact to the control of COVID-19 on campus.

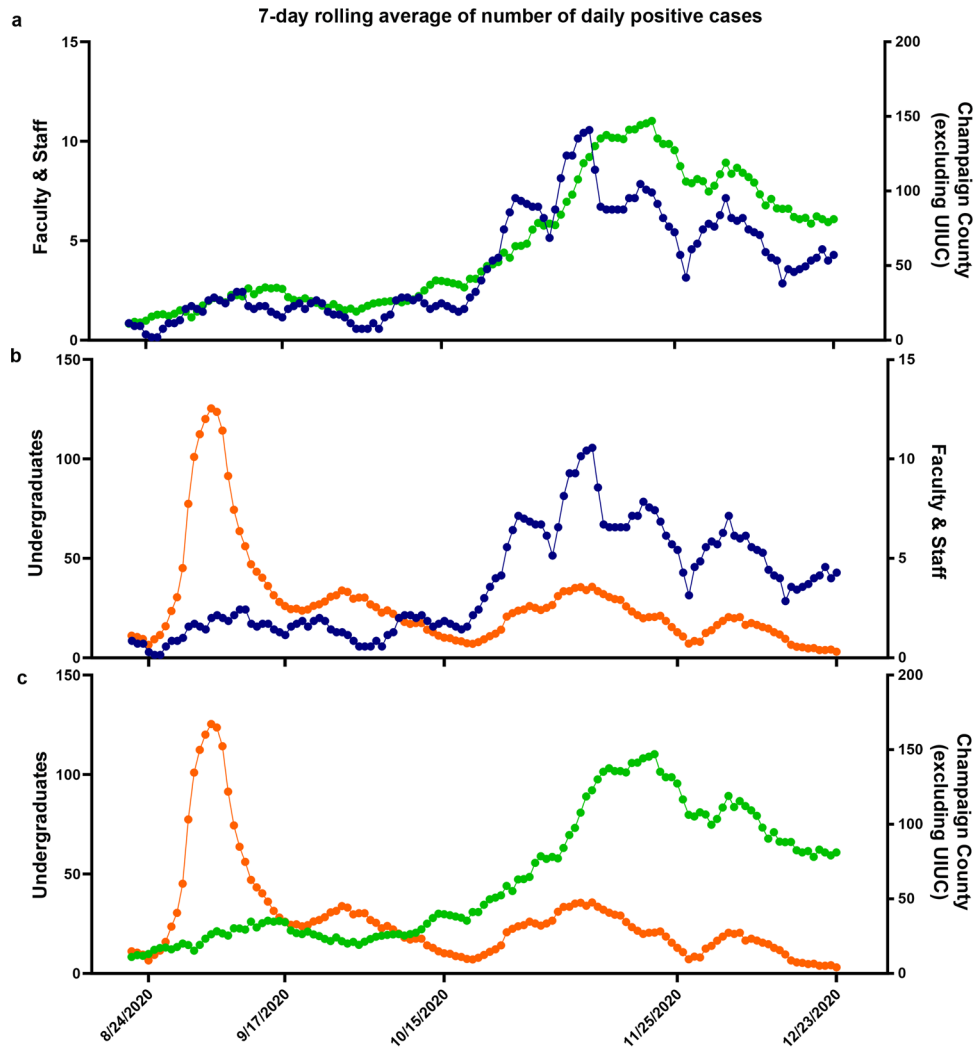


Fig. 5 Mitigation of SARS-CoV-2 spread in the context of the larger Champaign-Urbana Community. The daily number of 7-day averaged daily new cases between faculty/staff and residents in Champaign County **a**, undergraduates and faculty/staff **b**, and undergraduate students and residents in Champaign County **c**, for the period between August 15 and December 23. All points in three plots are colored according to their categories (orange: undergraduate students, blue: faculty/staff, green: residents in Champaign County). Pearson correlation coefficient, 95% confidence interval, and *p*-values for two-tailed test were calculated using GraphPad Prism software.

This program also yielded a novel, scalable, saliva-based RT-qPCR assay for SARS-CoV-2 that bypasses RNA extraction and is highly sensitive for detecting infected individuals early in the disease and throughout the period of likely infectiousness. This case study at the University of Illinois at Urbana-Champaign showed that the covidSHIELD saliva test is highly scalable and easy to implement, allowing fast, frequent and accurate testing in a large community. Our data suggests that every other day testing is able to identify individuals at earlier stages of infections as indicated by lower average viral loads, and daily testing is even better. While daily testing may not be practical on scale, such high frequency testing may be appropriate for certain at-risk groups, including those in congregate living and high contact athletics.

Finally, we note that the viral dynamics of different strains of SARS-CoV-2 can vary considerably. For example, viral loads for the Delta variant appear to peak sooner and higher, and remain elevated for longer periods of time, consistent with a substantially increased level of infectiousness for this strain^{51–53}. Similarly, the Omicron variant spread extremely fast during December 2021 and January 2022 and is characterized by a much shorter mean generation time⁵⁴. To address such challenges, it may be important to adapt testing frequencies accordingly.

Methods

Agent-based modeling. We simulate the spread of the epidemic using a full-scale stochastic agent-based model (ABM), which tracks the movement and disease stage of a large number of individuals as they attend both academic functions (like classes, libraries, and study groups) and social events (including eating at restaurants, congregating at bars, and attending parties). The core of the model comprises a set of 46,850 individuals who each follow independent schedules, which specify how the agents should move between different physical locations or zones. When an agent enters a zone, a random position in the zone is selected and the agent is assumed to stay at this position until he/she leaves the zone.

The model base is augmented by an infection model, which defines how agents become infected and infect other agents. Supplemental modules for testing, contact tracing, and quarantine/isolation can be interfaced with the core model to compare the effectiveness of various mitigation strategies.

Infection model description. Motivated by the airborne transmission dynamics of COVID-19, we have adopted the concept of “infection quantum”, which is defined as the dose of airborne droplet nuclei required to cause infection in 63% of susceptible persons⁵⁵. We introduce a hybrid transmission model which decomposes the infectious droplets into two parts: (1) large droplets with sizes larger than 10 microns which stay within a circle of radius 2-m from an infected agent and only infect its neighbors within the circle; and (2) small airborne droplet nuclei with dimensions <10 microns which spread homogeneously over the zone. Accumulating more quanta corresponds to increasing the probability of being infected.

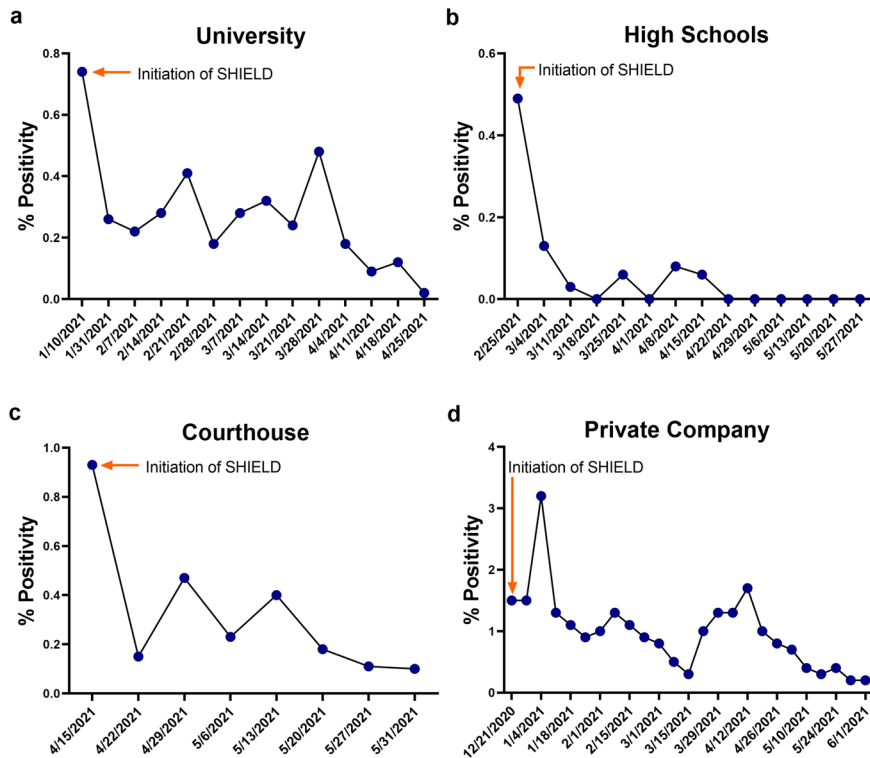


Fig. 6 Other communities with SHIELD. SHIELD was deployed at other locations in Winter 2020/Spring 2021. The results from four representative examples are shown: **a** a university (1x/week), **b** a pair of high schools (2x/week), **c** a courthouse (2x/week), and **d** a large private corporate campus (2x/week).

When an agent leaves a zone, they are infected with a probability that depends on the total number of quanta they accumulated in that zone = $\int n dt$. Specifically, the infection probability is given by

$$P[\text{infection}] = 1 - \exp(-m \times IR \times N) \tag{1}$$

where m is a modifier that accounts for modulation of inhaled quanta due to factors such as mask wearing, and IR is the inhalation rate of the susceptible individual⁵⁵.

The quanta emission rate from an infectious agent depends on their activities in different zones. For example, since students mostly stay silent during classes, the emission rate is estimated to be 4 quanta per hour. As a comparison, since agents often speak loudly in bars/parties, the quanta emission rate is assumed to be 150 quanta per hour. The emission rates are derived from Linsey et al.⁵⁶. In addition, the quanta emission rate is proportional to the infectiousness of the infected agent which vary with the in-host viral dynamics. The infectiousness starts to be non-zero after 2 days from the time exposure. This is mean latent period estimated for COVID-19. The infectiousness profile utilized in the model is obtained from a within-host model for COVID-19 that was calibrated by measurements of viral load dynamics²⁴.

The droplets exhaled by infected agents containing infectious viral particles are coarsely divided into two components based on the size of droplets: small airborne droplets ($\leq 10 \mu\text{m}$ in diameter) and large droplets ($> 10 \mu\text{m}$ in diameter). The small airborne droplets can suspend in the air for long periods of time due to the limited influence of gravity³⁷. As a result, airborne droplets are heavily influenced by the ventilation rate of the zone and a high ventilation rate can effectively reduce the transmission risk as will be discussed shortly. Since the small droplets spread over the entire zone (depends on the volume of the zone), viruses within exhaled infected agents can infect susceptible agents far away from infectors, and thus lead to long-range infections. The large droplets fall quickly to the ground due to gravity and thus spread only over a limited distance away from the infectious agent (typically $< 2 \text{m}$), making only short-range infections possible. The ratio of infectious viral particles between large droplets and airborne droplets f is adjusted to reproduce an observed initial doubling time of unmitigated epidemic equal to 2.5 days. This doubling time is motivated by observations of growth rate in COVID-19 cases in Chicago during February/early March 2020. The value of f used in this study is equal to 3.

Viral quanta cumulated from either large or small droplets are denoted as $n_{\text{short-range}}(t)$ and $n_{\text{long-range}}(t)$ respectively. Small droplets spread over a longer distance and are eventually well-mixed over the zone modulated by the ventilation:

$$\frac{dn_{\text{long-range}}(t)}{dt} + r_{\text{vent}} n_{\text{long-range}}(t) = \frac{\sum_i E_i}{V}, \tag{2}$$

where r_{vent} is the ventilation rate, i loops over all infected agents, and V is the volume of the zone.

Large droplets follow equations for short-range transmission dynamics modulated by both ventilation and gravity:

$$\frac{dn_{\text{short-range}}(t)}{dt} + (r_{\text{gravity}} + r_{\text{vent}}) n_{\text{local}}(t) = \frac{\sum_{i, < 2\text{m}} f E_i}{V_{\text{local}}}, \tag{3}$$

where r_{gravity} is the inverse of mean duration that large droplets stay in the air, i loops over all infected agents within 2-m range of the susceptible, and $V_{\text{short-range}}$ is the volume of a cylinder with radius 2 m and height 2 m. To simplify the computation, $n_{\text{short-range}}(t)$ is assumed to be in a steady state and thus

$$n_{\text{short-range}}(t) = \frac{\sum_{i, < 2\text{m}} f E_i}{(r_{\text{gravity}} + r_{\text{vent}}) V_{\text{local}}} \tag{4}$$

The quanta emission rates for different agents in various zones are described in Supplementary Table 8.

For each susceptible agent, the probability of being infected for each zone is independent. The infection probability for one susceptible in a zone depends on the accumulated quanta N and N is a time-integral of

$$n(t) = n_{\text{long-range}}(t) + n_{\text{short-range}}(t). \tag{5}$$

The disease transmission dynamics in homes/dorm environments is hard to be modeled for two reasons: (1) the unknown co-habitation information of agents and (2) too many independent houses/homes/dorm rooms to be tracked. This causes computational complexity. To consider the disease transmission due to cohabitation at homes/dorms, all agents in the simulation are grouped into pairs and they are roommates to each other. The disease transmission can happen between two roommates and the probability is computed from the quanta emission rate for breathing, the volume in typical dormitories, and the ventilation rate in dorms. For each night, an infection event between one susceptible roommate and the other infected roommate is probabilistic.

Schedules. Agents' schedules are generated before running the simulation and are motivated by real information about both undergraduate and graduate students' class schedules of the semester Fall 2019 as provided by the University of Illinois at Urbana-Champaign. A schedule comprises a list of zones and times that define where an agent should be as a function of time. To adapt for the agent-based model, the duration of classes is assumed to have a granularity of 30 min. Zones are divided into groups according to their function, and may be associated with academic courses, libraries or study groups, cafes, restaurants, or bars/parties. Each zone has a defined, static size and is associated with certain quanta emission rates

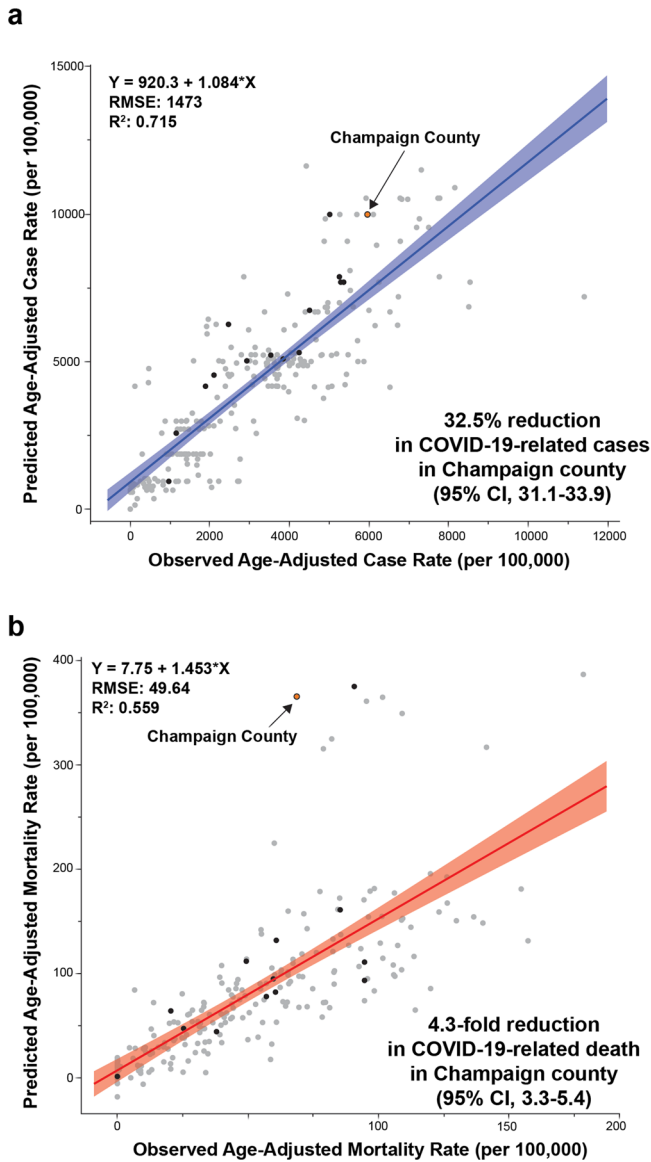


Fig. 7 Other communities without SHIELD. **a** and **b** Relationship between observed and predicted COVID-19 cases and mortality among counties with large university enrollments (student enrollment > 15,000 at start of Fall 2020 semester, $n = 251$). Predicted COVID-19 case and mortality rates were analyzed with a 3-week lag (to adjust for delays between exposure and outcome) using each county's social vulnerability index (SVI) and age-adjusted COVID-19 mortality, accounting for state (due to policy differences in COVID-19 management). COVID-19 human case data^{63,64} and SVI were provided from CDC (2021) and population data was provided from the U.S. Census Bureau (2019)⁶⁴. The lines indicate the fit lines for the linear regressions, with shaded areas indicating the 95% confidence intervals around the fits and circles indicating observations with Champaign County shown in orange and other Big 10 Conference Universities ($n = 16^*$) in black. *Hennepin and Ramsey Counties (MN) were both used for University of Minnesota.

(see Supplementary Table 8), e.g., the emission of quanta is higher in bars than classrooms since one is more likely to be talking in a bar. Besides the student population, there are also non-student agents (1 professor for every class and 5 workers in every bar, restaurant, cafe, or library). These other agents are assumed to stay at home for most of time except going to their working zones. There are assumed to be 15,000 students living in 300 dormitories, while the remaining students are divided into the other home zones. For simplicity, 300 dormitories are assumed to be the same size, with 50 students living in each one. The total number of non-student agents is 2446.

The disease transmission at home/dorm is assumed to be stochastic and it occurs between randomly paired roommates with a constant probability that is inferred from extended exposure overnight constrained by the typical volume and the ventilation rate of dormitories.

Although our assignment of courses is based on a real schedule, we can only synthesize the agents' out-of-school schedules. We use the following model to fill in the blanks:

- Agents are assumed to be home/dorm between 21h00 and 8h00.
- Agents do not skip classes.
- Agents eat at restaurants twice a day for lunch and dinner between (10–14 h) and (17 and 21 h), respectively. An agent will spend a random amount of time at the restaurant or dining home:

Lunch: uniform random between 0.5 and 1 h.
 Dinner: uniform random between 0.5 to 2 h.

- Agents who stay at home/dorm, in the library, at a cafe, or go to bars tend to stay a long time and the assumed time interval spent is given in Supplementary Table 9.
- 7000 students would go to bars after 6 p.m., and agents who go to bars/parties only do so on Thursdays and weekends. (Agents may stay overnight in bars).
- On a daily basis:

2500 agents would go to cafes if they are free at the time.

11250 students would go to libraries or congregate in study groups if they are free at the time.

5 out of 50 students living in each dormitory would go to a dorm party each night for 2 h.

- Agents would stay at home/dorm for a while if they have nothing else to do at the time.

To simulate the real-world campus, the schedule also added two groups of specialized agents: professors/staff and workers. Each course section is assigned with a course staff who would teach that section and stay at that class zone during class time. Each non-class zone (except home/dorm zone and lab zone) would have 5 workers who would stay at their working zone from 8 a.m. to 9 p.m. Workers will go for lunches and dinners as everyone else and this provides an opportunity for mixing between students and non-student agents.

In addition to the above specified in-semester schedules of all agents, we have also incorporated a pre-semester schedule that reflects student activities during the move-in week before the start of the semester. This is crucial because some agents may come to campus already infected and hence they will be detected by testing during initial screening and may also be capable of infecting other susceptible individuals while the mitigation strategies (such as mask-wearing and hybrid classes) are not fully effective yet. We have summarized our calculation for entry screening in an earlier report⁵⁸. Given the prevalence of COVID-19 in Illinois in August 2020, we estimated that approximately 300 infected agents will be detected in entry screening⁵⁸. In the 3-day pre-semester period, agents spend more time in restaurants, cafes, and bars. All agents are required to receive a universal testing screening in the next 2 days upon campus arrival.

Quarantine and isolation. Agents who are test positive will have their regular schedules modified through mandatory isolation and thus will be disconnected from the general population. Potentially exposed individuals are also identified through contact tracing and may be disconnected from the general population through mandatory quarantine. Thus, in our model, individuals may be disconnected from the population due to two reasons: (1) they have been confirmed as infected by testing. We call them: *isolated*. Or (2) they have not been confirmed yet but they might have been exposed to an infectious individual and are identified through contact tracing. We call them *quarantined*.

In the real world, quarantine can happen for a variety of reasons including either self-quarantine (e.g., following self-identification of symptoms) or as the result of manual contact tracing or exposure notification (where someone is directed to isolate because they have recently been in contact with an infected individual). In our model, to consider the worst-case scenario, we ignore the case of self-quarantine and attribute the quarantine to the manual contact tracing or exposure notification following an index case (i.e. a positive case). Individuals are quarantined following the manual contact tracing procedure from CDC and exposure notification procedure specified in the Safer Illinois exposure notification app utilized in UIUC. Individuals who are identified as close contacts of an index by manual contact tracers are quarantined for 14 days. If they show any symptoms during the 14-day quarantine period and are tested positive, they will be switched to an isolation protocol. Besides, individuals may be notified by the exposure notification app if their risk scores are larger than a certain threshold. Those individuals notified by the app will be quarantined for 5 days before receiving a test.

Testing. The testing module enables agents to be checked for the disease and be isolated from the general population if the testing procedure identifies them as having been infected. Our implementation of testing makes several assumptions:

Testing is only available for part of the day (between 8 a.m. and 6 p.m.). An infected agent may be incorrectly tested negative. For this modeling exercise, the false negative rate was assumed to be 11.1% based on initial studies³⁶. The false negative rate is likely much lower: In the clinical study shown in Fig. 2c, negative percent agreement for covidSHIELD assay with nasal swab-based assay was 98.9% (95% CI, 93.9–99.9%). The false positive rate of the test was assumed to be zero. The delay between having been tested and receiving the results of the test is 5 h. The testing results of all collected testing samples will be notified as soon as possible without the working hour limit.

Contact tracing and exposure notification. We implement modules for both manual contact tracing and automatic app-based exposure notification. The manual contact tracing is performed by manual contact tracers. Once an index case is identified by the test, the manual contact tracing starts to find the index's close contacts (i.e., contacts whose distance to the index is <2 m) staying more than 15 min with the index case. Given the fact that such a manual contact tracing requires a large force of manual contact tracers and not every close contact cannot be accurately identified, here we assume that only 50% of close contacts may be successfully traced. Close contacts in classes are hard to be identified due to random mixing that may happen between students. As a result, the whole class will be moved online and all agents in this class are quarantined once an infected case is diagnosed in this class.

The exposure notification (EN) function is modeled on the Privacy-Preserving Contact Tracing procedure developed by Apple and Google. The Safer Illinois version of this function, developed at UIUC, is a decentralized protocol that combines a smart phone's Bluetooth technology with privacy-preserving cryptography. The app emits Rolling Proxy Identifiers, or keys, multiple times per minute. These keys are randomly generated three or four times per hour. Keys are exchanged among phones that come within 2 m for a minimum amount of time. Keys that are emitted and keys that are sensed are stored locally on individual phones. When the owner of a phone tests positive for SARS-CoV-2, an encrypted notification is sent to a central server along with all of the keys that person's phone emitted during the past 3 days. These keys cannot reveal the identity of the person who tested positive or the location where someone may have been exposed. The encrypted keys of confirmed cases are automatically downloaded via the app by all users and are compared to the saved keys on a person's phone. Whenever there is a match between the encrypted keys of confirmed cases and locally saved keys, the risk score of the user is updated. If the total risk score of the user in the past 14 days is larger than a threshold, the user is notified by the exposure notification system in the Safer Illinois app.

We enhance the exposure notification through a risk-weighted approach. The probability of being infected depends on three factors: infectiousness of the index, contact duration, and the zone risk. Thus, the risk-weighted protocol is developed here to reflect these factors in the risk score. The risk score is defined as contact duration (in hours) with all index cases weighted by the infectiousness of all index cases. The infectiousness is scaled to make the peak infectiousness as 1. Given the probability of being infected in zones such as bars is much higher than the infection probabilities in all other zones, the risk score in such risky zones is increased to reflect the true process of disease transmission. To achieve this, all agents' activities during weekends' and Thursdays' nights will be treated as in bars and their risk scores are multiplied by 10. The notification happens when the total risk score passes 2.

Additional mitigation strategies. In addition to the testing, contact tracing, and exposure notification, there are several extra mitigation strategies effective for reducing the infection:

Hybrid classes: a fraction of classes (especially large classes) is moved online to reduce the contact hours between students. In the model, all classes with the size over 50 are moved online and all students are assumed to stay at home/dorm when they are taking the online class.

Mask-wearing: masks can reduce both the emission rate and the inhaled rate of viral quanta. In our model, the overall reduction coefficient for the mask-wearing is assumed to be 50% when both the infector and infectee wear masks. The mask efficiency in reducing emission is assumed to be 30%. The mask efficiency in reducing inhalation is assumed to be 30%. These numbers are conservatively assumed consistent with a single layer cloth mask. Thus, if either the infector or the susceptible individuals does not wear a mask, the mask reduction in transmission is only 30%. If both agents wear masks, the effect of masking is quadratic and the transmission is reduced by $(1-0.3)^2 = 0.49$, or ~50%.

Evaluating the multiplier, M , for testing frequency. We adopted the following infectiousness profile, after Goyal et al. (2020)²⁴, which includes 2-day latency

period of [0.0, 0.0, 0.148, 1.0, 0.823, 0.426, 0.202, 0.078, 0.042, 0.057, 0.009, 0.0, 0.0, 0.0, 0.0, 0.0]. The sum of this infectiousness list is therefore 2.785. The effect of testing frequency on reducing the transmission chain may be estimated as follows:

A. Testing once a week:

With one test a week, agents may test positive and get isolated on days 3, 4, 5, 6, 7, 8 or 9 after exposure with a probability = 1/7. Therefore, the expected sum of infectiousness profile modulated by 1 test a week is $(1/7)*0.148 + (1/7)*(0.148 + 1.0) + (1/7)*(0.148 + 1.0 + 0.823) + (1/7)*(0.148 + 1.0 + 0.823 + 0.426) + (1/7)*(0.148 + 1.0 + 0.823 + 0.426 + 0.202) + (1/7)*(0.148 + 1.0 + 0.823 + 0.426 + 0.202 + 0.078) + (1/7)*(0.148 + 1.0 + 0.823 + 0.426 + 0.202 + 0.078 + 0.042) = 1.951$. This generates a R_0 multiplier = $1.951/2.785 = 70.5\%$.

B. Testing two times a week:

With two tests a week, agents may test positive and get isolated on days 3, 4, or 5 after exposure with a probability = 2/7, while agents may test positive and get isolated 5.5 days after exposure with a probability = 1/7. Therefore, the expected sum of infectiousness profile modulated by 2 tests a week is $(2/7)*0.148 + (2/7)*(0.148 + 1.0) + (2/7)*(0.148 + 1.0 + 0.823) + (1/7)*(0.148 + 1.0 + 0.823 + 0.426 + 0.202 + 0.078) + (1/7)*(0.148 + 1.0 + 0.823 + 0.426 + 0.202 + 0.078 + 0.042) = 1.245$, generating a R_0 multiplier = $1.245/2.785 = 44.7\%$.

Computation of R_0 in the hybrid transmission model. In the hybrid transmission model, the infection occurs through the accumulation of infectious quanta emitted from all infectious agents present in the zone. In other words, the concept of transmission pair is not clear and instead, each infectious agent has a fractional contribution to an infection event. As a result, here we attempt to estimate R_0 as a sum of fractional contributions. First, for each infection event that occurred in the simulation, we recorded the infection zone and time for this individual and obtained all infectious agents within the zone at that time according to the schedule and excluded all isolated agents. Second, for an infection event with n infectors, we assigned a fractional R_0 contribution $1/n$ for each infector. Finally, during the early period of the epidemic, the fractional R_0 for all infection events are assigned to all infectious agents in presence, and R_0 for each infected agent is a sum of all fractional R_0 .

Estimating the effective reproduction number based on daily new cases on campus. We computed the time-dependent effective reproduction number and growth rate throughout the fall semester accounting for variability in testing frequency and reporting delays (Fig. 4 in the main text). The calculations were done using the package EpiNow2 which implements a range of open-source tools⁴⁶, and current best practices⁴⁷.

In using the package, we have made the following assumptions:

- The all-time mean and median of test results reporting delays on campus are 9.29 and 8.34 h, respectively. These are much shorter than the typical reporting delays in testing of the general public (48–72 h).
- Under-reporting is neglected. The test uptake on campus was near universal. Everybody was required to test and those who did not comply was subject to disciplinary action. Therefore, we were detecting, in principle, all the cases and the undetected cases, if any, were negligible.
- The time between two consecutive tests was approximately distributed according to the data shown in Supplementary Fig. 7 with the mean and standard deviation equal to 4.14 and 3.4 days, respectively.
- The generation time is assumed to be gamma distributed consistent with the data from Ganyani et al. (2020)⁵⁹.

Acquisition and processing of clinical samples. All clinical samples from study participants were collected in accordance with Western IRB-approved protocol number 20203538. Participants were recruited from populations seeking SARS-CoV-2 tests and were included if they (1) reported symptoms consistent with COVID-19 or suspected exposure to an infected individual, (2) had never tested positive for SARS-CoV-2, (3) were at least 18 years of age, and (4) spoke English. All participants provided informed consent at the time of recruitment. Analysis of aggregate data from campus was ruled exempt by the University of Illinois Urbana-Champaign Institutional Review Board, protocol number 21,216. Participants provided a 2 mL saliva sample, and a health professional collected a nasopharyngeal swab following standard procedures. The saliva sample was transported to the Veterinary Diagnostic Laboratory within 24 h for analysis following the outlined procedure. The nasopharyngeal swab was inserted into viral transport media and stored at -80°C until analysis with an FDA-approved comparator at an independent diagnostic laboratory.

Supplementary Table 5 summarizes the method comparison study completed to support the correlation between saliva samples processed with covidSHIELD and nasal samples processed with Abbott RealTime SARS-CoV-2 assay performed on the Abbott m2000 System. Supplementary Table 6 outlines the details to capture on case report form. Supplementary Table 1 summarizes the 25 clinical samples were split into two aliquots upon receipt, one set was processed using our covidSHIELD assay and the other set was subjected to RNA extraction using MagMax Viral/

Pathogen II (MVP II) Nucleic Acid Isolation Kit (ThermoFisher CN A48383). 5 μ L of either processed saliva (in 1:1 2 \times TBE/Tween-20 buffer) or purified RNA (in water) were subsequently used as templates for RT-qPCR. Supplementary Table 7 summarizes the comparative study of mid-turbinate (MT) swab and saliva from 17 individuals identified with low viral load based on MT swab analyzed using Abbott Alinity RT-PCR at the Johns Hopkins University School of Medicine. Contemporaneously collected saliva samples from the same individuals were analyzed using the covidSHIELD assay at the University of Illinois Urbana-Champaign CLIA-registered laboratory.

SARS-CoV-2 inactivated virus. In most experiments, fresh pooled saliva were spiked with gamma-irradiated (BEI cat# NR-52287, Lot no. 70033322) SARS-CoV-2 virions. SARS-Related Coronavirus 2, Isolate USA-WA1/2020, Gamma-irradiated, NR-52287 was deposited by the Centers for Disease Control and Prevention and obtained through BEI Resources, NIAID, NIH. The reported genome copy number pre-inactivation for γ -irradiated SARS-CoV-2 is 1.7×10^9 genome equivalents/mL for the specified lot number. All virus stocks were aliquoted in small volumes and stored at -80°C . Stocks were serially diluted to the correct concentration in RNase-free water on the day of experimentation.

Collection and processing of fresh saliva from healthy donors for Limit of Detection (LoD) assay. Fresh saliva was collected from healthy individuals in 50 mL conical tubes (BD Falcon/Corning 352098) in accordance with University of Illinois at Urbana-Champaign IBC-approved protocol numbers 4604 and 4589. Known amounts of the SARS-CoV-2 inactivated virus (BEI cat# NR-52287) were spiked into saliva samples. Samples were processed according to the covidSHIELD instructions for use (<https://www.fda.gov/media/146317/download>). Briefly, samples were incubated in a hot water bath at 95°C for 30 min. After cooling the sample on ice, 100 μ L saliva was transferred to 96-deep-well plates pre-loaded with 100 μ L of 2 \times TBE (ThermoFisher CN AM9863) + 1% Tween-20 (ThermoFisher CN AM9863) buffer at 1:1 dilution ratio. 5 μ L of this sample preparation was used as template for RT-qPCR reactions.

We performed a multiplex RT-qPCR assay using the TaqPath RT-PCR COVID-19 kit (ThermoFisher CN A47814) together with the TaqPath 1-step master mix—No ROX (ThermoFisher CN A28523). All RT-qPCR reactions, comprised of 5 μ L template + 5 μ L of reaction mix (2.5 μ L TaqPath 1-step master mix, 0.5 μ L TaqPath primer/probe mix, 1.0 μ L MS2, and 1.0 rnase-free water), were performed in 384-well reaction plates in a QuantStudio 7 system (Applied Biosciences). The RT-qPCR was run using the standard mode, consisting of a hold stage at 25°C for 2 min, 53°C for 10 min, and 95°C for 2 min, followed by 40 cycles of a PCR stage at 95°C for 3 s then 60°C for 30 s; with a 1.6°C/s ramp up and ramp down rate. The limit of detection (LoD) of the assay was performed by serial dilution of γ -irradiated SARS-CoV-2 ($0-5.0 \times 10^5$ viral copies/mL) used to spike pooled fresh saliva samples. LoD experiments were repeatedly performed at least five times in different machines.

In some experiments, the CDC-approved assay was used to validate our data using the TaqPath 1-step mix (ThermoFisher CN A15300). Primers and probes targeting the *N1*, *N2*, and *RNase P (RP)* genes were purchased from Integrated DNA Technologies as listed: nCOV_N1 Forward Primer Aliquot (CN 10006830), nCOV_N1 Reverse Primer Aliquot (CN 10006831), nCOV_N1 Probe Aliquot (CN 10006832), nCOV_N2 Forward Primer Aliquot (CN 10006833), nCOV_N2 Reverse Primer Aliquot (CN 10006834), nCOV_N2 Probe Aliquot (CN 10006835), RNase P Forward Primer Aliquot (CN 10006836), RNase P Reverse Primer Aliquot (CN 10006837), RNase P Probe Aliquot (CN 10006838). The 2019-nCoV_N_Positive Control (IDT CN 10006625) was used as positive control at 50 copies/ μ L dilution. LoD experiments using CDC primers were performed at least three times.

RT-qPCR data analysis. Following completion of RT-qPCR, data were processed using QuantStudio Design and Analysis Software (version 2.4.3) with a threshold setting of 10,000 and a baseline setting of 5. Cycle threshold (Ct) cut-off was set at 39. Ct values were plotted as single replicate values on a scatter plot, using GraphPad Prism 9 (version 9.3.1).

SHIELD deployment in other communities. Saliva samples were collected from a large public university, a pair of high schools, a federal courthouse, and a large private corporate campus. Samples were processed and analyzed using the covidSHIELD assay (FDA EUA 202555). The test results were evaluated according to the interpretation tables in the EUA Summary (<https://www.fda.gov/media/146317/download>). The weekly averaged positivity rates are plotted against the period the samples were processed.

Development of Safer Illinois app. Prior to the COVID-19 pandemic, a large collaborative effort led by the Safe, Healthy Community Initiative on campus had been developing an open source software platform called Rokwire⁶⁰. Rokwire is designed to make it easy for individuals and organizations to build apps for mobile devices that support smarter, healthier communities. We had been using the University of Illinois at Urbana-Champaign campus as a test bed for the development of Rokwire—the platform—and the first app built upon it—the Illinois

app. Safer Illinois was built on the Rokwire platform and the source code was made open source August 14, 2020⁶¹.

As part of the process of designing Safer Illinois, we met with and sought feedback from a diverse set of stakeholders: faculty and students, mental health advocates, leadership in Student Affairs, the Faculty Senate, the Graduate Employees Organization, and a range of individuals with expertise in digital privacy. Collectively, these groups expressed a variety of concerns related to privacy and data security.

We took multiple actions to address the concerns expressed. We built privacy into Safer Illinois from the ground up. We made modifications to a beta version of the app to minimize the data we collected and stored so that collected only the data necessary to allow the app to function. We designed the app to store data related to Exposure Notification for the shortest possible period and then delete it. We ensured that users could delete their data at any time from both the app and servers. We made our privacy notice novice friendly, so that all consent language allowed users to understand up front exactly what data we collect, what we do with that data, how long we keep it, and how users can manage their data⁶¹.

Reporting summary. Further information on research design is available in the Nature Research Reporting Summary linked to this article.

Data availability

Aggregate case and testing data are publicly available at <https://go.illinois.edu/COVIDTestingData>. Analysis of aggregate data from campus was ruled exempt by the University of Illinois Urbana-Champaign Institutional Review Board, protocol number 21216. All other data may be requested through the COVID Research Oversight Committee at <https://redcap.link/crocdatasamples>. Link to the code for analysis of county-level mortality in the BigTen: https://github.com/juel15401/Big10UniversityCounties_COVID.git. <https://doi.org/10.5281/zenodo.6481689>

Code availability

Source code repository of “Safer Illinois” App - the official COVID-19 app of the University of Illinois: <https://github.com/rokwire/safer-illinois-app>⁶¹. <https://doi.org/10.5281/zenodo.6493203>

Received: 13 October 2021; Accepted: 19 May 2022;

Published online: 09 June 2022

References

- Morawska, L. & Milton, D. K. It is time to address airborne transmission of coronavirus disease 2019 (COVID-19). *Clin. Infect. Dis.* **71**, 2311–2313 (2020).
- Tkachenko, A. V. et al. Stochastic social behavior coupled to COVID-19 dynamics leads to waves, plateaus, and an endemic state. *eLife* **10**, e68341 (2021).
- Weitz, J. S., Park, S. W., Eksin, C. & Dushoff, J. Awareness-driven behavior changes can shift the shape of epidemics away from peaks and toward plateaus, shoulders, and oscillations. *Proc. Natl Acad. Sci. USA* **117**, 32764 (2020).
- Richmond, C. S., Sabin, A. P., Jobe, D. A., Lovrich, S. D. & Kenny, P. A. SARS-CoV-2 sequencing reveals rapid transmission from college student clusters resulting in morbidity and deaths in vulnerable populations. Preprint at *medRxiv* <https://doi.org/10.1101/2020.10.12.20210294> (2020).
- Wilson, E. et al. Multiple COVID-19 clusters on a University Campus—North Carolina, August 2020. *Mmwr. Morb. Mortal. Wkly. Rep.* **69**, 1416–1418 (2020).
- Korn, M. et al. Coronavirus pushes colleges to the breaking point, forcing ‘hard choices’ about education. *Wall Street J. (Online)* <https://www.wsj.com/articles/coronavirus-pushes-colleges-to-the-breaking-point-forcing-hard-choices-about-education-11588256157> (2020).
- Weeden, K. & Cornwell, B. The small-world network of college classes: implications for epidemic spread on a university campus. *Sociol. Sci.* **7**, 222–241 (2020).
- Gressman, P. T. & Peck, J. R. Simulating COVID-19 in a university environment. *Math. Biosci.* **328**, 108436–108436 (2020).
- Paltiel, A. D., Zheng, A. & Walensky, R. P. Assessment of SARS-CoV-2 Screening Strategies to Permit the Safe Reopening of College Campuses in the United States. *JAMA Network Open* **3**, e2016818–e2016818 (2020).
- Lopman, B. et al. A modeling study to inform screening and testing interventions for the control of SARS-CoV-2 on university campuses. *Sci. Rep.* **11**, 1–11 (2021).
- Renner, L., Kalbaugh, C. A., Shi, L. & McMahan, C. Modelling the impact of presymptomatic testing on COVID-19 outbreaks in university campuses. *BMJ Open* **10**, e042578 (2020).

12. Bansal, S. et al. There is no safe way to reopen colleges this fall: reopening colleges during a pandemic is too dangerous. *Wash. Post* <https://www.washingtonpost.com/outlook/2020/06/30/there-is-no-safe-way-reopen-colleges-this-fall/> (2020).
13. Frazier, P. I. et al. Modeling for COVID-19 college reopening decisions: Cornell, a case study. *Proc. Natl Acad. Sci. USA* **119**, <https://doi.org/10.1073/pnas.2112532119> (2022).
14. Johansson, M. A. et al. SARS-CoV-2 transmission from people without COVID-19 symptoms. *JAMA Netw. Open* **4**, e2035057 (2021).
15. Ye, F. et al. Delivery of infection from asymptomatic carriers of COVID-19 in a familial cluster. *Int. J. Infect. Dis.* **94**, 133–138 (2020).
16. Shental, N. et al. Efficient high-throughput SARS-CoV-2 testing to detect asymptomatic carriers. *Sci. Adv.* **6**, eabc5961 (2020).
17. Furukawa, N. W., Brooks, J. T. & Sobel, J. Evidence supporting transmission of severe acute respiratory syndrome coronavirus 2 while presymptomatic or asymptomatic. *Emerg. Infect. Dis.* **26**, <https://doi.org/10.3201/eid2607.201595> (2020).
18. Li, R. et al. Substantial undocumented infection facilitates the rapid dissemination of novel coronavirus (SARS-CoV-2). *Science* **368**, 489–493 (2020).
19. He, X. et al. Temporal dynamics in viral shedding and transmissibility of COVID-19. *Nat. Med.* **26**, 672–675 (2020).
20. Larremore, D. B. et al. Test sensitivity is secondary to frequency and turnaround time for COVID-19 screening. *Sci. Adv.* **7**, eabd5393 (2021).
21. Wölfel, R. et al. Virological assessment of hospitalized patients with COVID-2019. *Nature* **581**, 465–469 (2020).
22. Tan, W. et al. Viral kinetics and antibody responses in patients with COVID-19. Preprint at *MedRxiv* <https://doi.org/10.1101/2020.03.24.20042382> (2020).
23. Zhou, R. et al. Viral dynamics in asymptomatic patients with COVID-19. *Int. J. Infect. Dis.* **96**, 288–290 (2020).
24. Goyal, A., Reeves, D. B., Cardozo-Ojeda, E. F., Schiffer, J. T. & Mayer, B. T. Viral load and contact heterogeneity predict SARS-CoV-2 transmission and super-spreading events. *Elife* **10**, <https://doi.org/10.7554/eLife.63537> (2021).
25. Kissler, S. M. et al. Viral dynamics of acute SARS-CoV-2 infection and applications to diagnostic and public health strategies. *PLoS Biol.* **19**, e3001333 (2021).
26. Wang, C. C. et al. Airborne transmission of respiratory viruses. *Science* **373**, <https://doi.org/10.1126/science.abd9149> (2021).
27. Ferretti, L. et al. Quantifying SARS-CoV-2 transmission suggests epidemic control with digital contact tracing. *Science* **368**, <https://doi.org/10.1126/science.abb6936> (2020).
28. Han, P. & Ivanovski, S. Saliva—friend and foe in the COVID-19 outbreak. *Diagnostics* **10**, 290 (2020).
29. Sharma, S., Kumar, V., Chawla, A. & Logani, A. Rapid detection of SARS-CoV-2 in saliva: can an endodontist take the lead in point-of-care COVID-19 testing? *Int. Endod. J.* **53**, 1017–1019 (2020).
30. Braz-Silva, P. H., Pallos, D., Gianecchini, S. & To, K. K. W. SARS-CoV-2: What can saliva tell us? *Oral Dis.* <https://doi.org/10.1111/odi.13365> (2020).
31. Wyllie, A. L. et al. Saliva or Nasopharyngeal Swab Specimens for Detection of SARS-CoV-2. *N. Engl. J. Med.* **383**, 1283–1286 (2020).
32. Iwasaki, S. et al. Comparison of SARS-CoV-2 detection in nasopharyngeal swab and saliva. *J. Infect.* **81**, e145–e147 (2020).
33. Czumbel, L. M. et al. Saliva as a candidate for COVID-19 diagnostic testing: a meta-analysis. *Front. Med. (Lausanne)* **7**, 465 (2020).
34. Pasomsub, E. et al. Saliva sample as a non-invasive specimen for the diagnosis of coronavirus disease 2019: a cross-sectional study. *Clin. Microbiol. Infect.* **27**, 285.e281–285.e284 (2021).
35. Butler-Laporte, G. et al. Comparison of saliva and nasopharyngeal swab nucleic acid amplification testing for detection of SARS-CoV-2: a systematic review and meta-analysis. *JAMA Intern. Med.* **181**, 353–360 (2021).
36. Ranao, D. R. E. et al. Saliva-based molecular testing for SARS-CoV-2 that bypasses RNA extraction. Preprint at *bioRxiv* <https://doi.org/10.1101/2020.06.18.159434> (2020).
37. Batéjat, C., Grassin, Q., Manuguerra, J.-C. & Leclercq, I. Heat inactivation of the severe acute respiratory syndrome coronavirus 2. *Cold Spring Harb. Lab.* <https://doi.org/10.1101/2020.05.01.067769> (2020).
38. Fomsgaard, A. S. & Rosenstjerne, M. W. An alternative workflow for molecular detection of SARS-CoV-2 – escape from the NA extraction kit-shortage, Copenhagen, Denmark, March 2020. *Euro Surveill.* **25**, <https://doi.org/10.2807/1560-7917.es.2020.25.14.2000398> (2020).
39. Vogels, C. B. F. et al. SalivaDirect: a simplified and flexible platform to enhance SARS-CoV-2 testing capacity. *Medicine* **2**, 263–280.e266, (2021).
40. Ke, R. et al. Daily longitudinal sampling of SARS-CoV-2 infection reveals substantial heterogeneity in infectiousness. *Nature Microbiology* **7**, 640–652, (2022).
41. Bullard, J. et al. Predicting infectious SARS-CoV-2 from diagnostic samples. *Clin. Infect. Dis.* <https://doi.org/10.1093/cid/ciaa638> (2020).
42. Vetter, P. et al. Daily viral kinetics and innate and adaptive immune response assessment in COVID-19: a case series. *mSphere* **5**, <https://doi.org/10.1128/mSphere.00827-20> (2020).
43. Perera, R. A. et al. SARS-CoV-2 virus culture from the upper respiratory tract: correlation with viral load, subgenomic viral RNA and duration of illness. Preprint at *medRxiv* <https://doi.org/10.1101/2020.07.08.20148783> (2020).
44. Cevik, M. et al. SARS-CoV-2, SARS-CoV, and MERS-CoV viral load dynamics, duration of viral shedding, and infectiousness: a systematic review and meta-analysis. *Lancet Microbe* **2**, e13–e22 (2021).
45. Gniazdowski, V. et al. Repeat COVID-19 molecular testing: correlation of SARS-CoV-2 culture with molecular assays and cycle thresholds. *Clin. Infect. Dis.* <https://doi.org/10.1093/cid/ciaa1616> (2020).
46. Abbott, S. et al. Estimating the time-varying reproduction number of SARS-CoV-2 using national and subnational case counts [version 2; peer review: 1 approved with reservations]. *Wellcome Open Res.* **5**, <https://doi.org/10.12688/wellcomeopenres.16006.2> (2020).
47. Gostic, K. M. et al. Practical considerations for measuring the effective reproductive number. *Rt. PLoS Comput. Biol.* **16**, e1008409 (2020).
48. Wallinga, J. & Lipsitch, M. How generation intervals shape the relationship between growth rates and reproductive numbers. *Proc. Biol. Sci.* **274**, 599–604 (2007).
49. Verity, R. et al. Estimates of the severity of coronavirus disease 2019: a model-based analysis. *Lancet Infect. Dis.* **20**, 669–677 (2020).
50. CDC SVI Documentation 2018. Agency for Toxic Substances and Disease Registry. https://www.atsdr.cdc.gov/placeandhealth/svi/documentation/SVI_documentation_2018.html (2020).
51. Li, B. et al. Viral infection and transmission in a large, well-traced outbreak caused by the SARS-CoV-2 Delta variant. *Nat. Commun.* **13**, 1–9 (2022).
52. Chia, P. Y. et al. Virological and serological kinetics of SARS-CoV-2 Delta variant vaccine breakthrough infections: a multicentre cohort study. *Clin. Microbiol. Infect.* **28**, 612.e1–612.e7 (2022).
53. Kang, M. et al. Transmission dynamics and epidemiological characteristics of Delta variant infections in China. Preprint at *medRxiv* <https://doi.org/10.1101/2021.08.12.21261991> (2021).
54. Abbott, S., Sherratt, K., Gerstung, M. & Funk, S. Estimation of the test to test distribution as a proxy for generation interval distribution for the Omicron variant in England. Preprint at *medRxiv* <https://doi.org/10.1101/2022.01.08.22268920> (2022).
55. Buonanno, G., Stabile, L. & Morawska, L. Estimation of airborne viral emission: quantification of emission rate of SARS-CoV-2 for infection risk assessment. *Environ. Int.* **141**, 105794 (2020).
56. Marr, L. et al. FAQs on protecting yourself from aerosol transmission. <http://tinyurl.com/faqs-aerosol> (2020).
57. Stetzenbach, L. D., Buttner, M. P. & Cruz, P. Detection and enumeration of airborne biocontaminants. *Curr. Opin. Biotechnol.* **15**, 170–174 (2004).
58. Elbanna, A. et al. Entry screening and multi-layer mitigation of COVID-19 cases for a safe university reopening. *Epidemiology* <https://doi.org/10.1101/2020.08.29.20184473> (2020).
59. Ganyani, T. et al. Estimating the generation interval for coronavirus disease (COVID-19) based on symptom onset data, March 2020. *Eur. Surveill.* **25**, 2000257 (2020).
60. Rokwire. *Safer Illinois App.* <https://rokwire.org> (2020).
61. Smart, Healthy Communities Initiative. *Safer Illinois (Version 2.12.8)* [Source Code] (Github, 2022).
62. Cori, A., Ferguson, N. M., Fraser, C. & Cauchemez, S. A new framework and software to estimate time-varying reproduction numbers during epidemics. *Am. J. Epidemiol.* **178**, 1505–1512 (2013).
63. Centers for Disease Control and Prevention. *COVID-19 Case Surveillance Restricted Data Access, Summary, and Limitations*. Surveillance Review Response Group (US Center for Disease Control (CDC), 2021).
64. The American Community Survey. *ACS Supplemental Estimates Detailed Tables*. (US Census Bureau, 2019).

Acknowledgements

We gratefully acknowledge University of Illinois at Urbana-Champaign for funding. UIUC has also received support from CIMIT through the POCTRN program. CIMIT and POCTRN are supported by the RADx Tech program and have been funded in part with federal funds from the National Institute of Biomedical Imaging and Bioengineering, National Institutes of Health, Department of Health and Human Services, under Grant No. U54EB015408 awarded to R.L.S. With this work we would like to remember our colleague and co-author Joseph Gregory Gulick who passed away during the late stage of this project. He made critical contributions to the success of the SHIELD program. We would also like to acknowledge Michael Vincent and Diana Yates (Public Affairs, College of Media, University of Illinois at Urbana-Champaign) for editorial support. This work was supported by the University of Illinois System Office, the Office of the Vice-Chancellor for Research and Innovation, the Grainger College of Engineering, and the Department of Physics at the University of Illinois at Urbana-Champaign. Z.J.W. is supported in part by the United States

Department of Energy Computational Science Graduate Fellowship, provided under Grant No. DE-FG02-97ER25308. A.E.I. acknowledges partial support by NSF CAREER Award No. 1753249. This work made use of the Illinois Campus Cluster, a computing resource that is operated by the Illinois Campus Cluster Program (ICCP) in conjunction with the National Center for Supercomputing Applications (NCSA) and which is supported by funds from the University of Illinois at Urbana-Champaign. This research was partially done at, and used resources of the Center for Functional Nanomaterials, which is a U.S. DOE Office of Science Facility, at Brookhaven National Laboratory under Contract No.~DE-SC0012704. This study was also partially funded by the National Institute for Biomedical Imaging and Bioengineering grant number U54EB027690, part of the National Institutes of Health.

Author contributions

M.D.B., P.J.H., T.M.F., R.L.S., N.D.G., W.C.S., J.T.W., S.A.M., A.C.C., R.J.J., and T.L.K. conceived, designed, and guided the research, M.D.B., P.J.H., T.M.F., R.L.S., N.D.G., W.C.S., A.E.I., and D.R.E.R. wrote the paper, M.D.B., P.J.H., T.M.F., N.D.G., R.L.S., W.C.S., A.E.I., J.T.W., C.B.B., A.V., S.A.M., A.C.C., R.J.J., T.L.K., K.C.W., K.W., R.S.W., E.V., S.V., E.A.T., M.A.T., R.T. M.S., C.Sm., T.H.S., C.Sk., J.M.S., A.S., M.E.S., L.N.R., E.R., M.L.R., J.R., J.Q., M.C.P., C.P., J.M.P., J.P., A.P., N.A.P., M.N., A.D.M., K.M., M.M., H.H.M., J.Mo., A.Mir., K.G.M., R.M., J.Ma., Y.C.M., R.L.L., L.M.K., T.K., A.K., P.K., I.J., N.I., A.A.H., A.H., R.M.H., A.G., B.G., D.G., S.A.G., N.Gas., N.Gal., B.W.F., D.F., J.F., T.E., A.Ed., J.E., M.Cu., M.Co., A.C., J.Bu., J.Bl., I.B., J.D.B., K.M.B., M.B., R.L.B., M.J.L., J.E.N., N.J.C., D.L.Y., M.H.L., G.S., J.C.C., M.G., J.S.M., R.B., J.A.V., J.L., W.E.W., D.B.Y., D.S.S., S.P.B., L.M., P.K.A., E.A.V., M.J., J.L.S., A.C.V., C.H., R.N.K., J.A.P., C.Si., J.Br., D.M.K., N.W., G.D., C.B.-P., B.R.B., L.W.-B., M.D.L., K.D., M.R.F.J., J.D.S., C.B., E.S., R.C.P.J., P.M.H., M.P.S., T.J.N., J.G., A.Mil., I.J.G., S.P.S. J.G.G., N.P.V., J.M.P., S.J.P., A.I., Z.L., H.Z., A.V.T., Z.J.W., S.M., J.U., G.N.W., T.W., R.L.F., L.W., K.J.G., F.G.A., R.L.H., and D.R.E.R. performed the research.

Competing interests

University of Illinois at Urbana-Champaign has filed two pending patent applications related to the saliva-based assay described herein (US Nonprovisional Application No. 17/350,670, filed June 17, 2021; US National Phase Application No. 17/636,469, filed on February 18, 2022), and D.R.E.R., R.L.H., F.G.A., K.J.G., L.W., C.R.B., M.D.B., T.M.F., and P.J.H. are co-inventors. S.J.P., J.M.P., W.C.S., R.J.J., and A.C.C. are associated with Rokwire, which created the Safer Illinois App. G.D. and N.W. are associated with TekMill

which created some of the automation used in the VDL COVID-19 Testing Lab at UIUC. P.J.H., A.C.C., S.A.M. and J.T.W. are Members of the Board of Managers for the University Related Organization SHIELD T3, LLC, which has obtained a non-exclusive license to this technology. The remaining authors declare no competing interests.

Additional information

Supplementary information The online version contains supplementary material available at <https://doi.org/10.1038/s41467-022-30833-3>.

Correspondence and requests for materials should be addressed to Ahmed Elbanna, William C. Sullivan, Rebecca L. Smith, Nigel Goldenfeld, Timothy M. Fan, Paul J. Hergenrother or Martin D. Burke.

Peer review information *Nature Communications* thanks the anonymous reviewer(s) for their contribution to the peer review of this work.

Reprints and permission information is available at <http://www.nature.com/reprints>






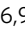





Publisher's note Springer Nature remains neutral with regard to jurisdictional claims in published maps and institutional affiliations.



Open Access This article is licensed under a Creative Commons Attribution 4.0 International License, which permits use, sharing, adaptation, distribution and reproduction in any medium or format, as long as you give appropriate credit to the original author(s) and the source, provide a link to the Creative Commons license, and indicate if changes were made. The images or other third party material in this article are included in the article's Creative Commons license, unless indicated otherwise in a credit line to the material. If material is not included in the article's Creative Commons license and your intended use is not permitted by statutory regulation or exceeds the permitted use, you will need to obtain permission directly from the copyright holder. To view a copy of this license, visit <http://creativecommons.org/licenses/by/4.0/>.

© The Author(s) 2022

Diana Rose E. Ranoa^{1,2,3}, Robin L. Holland⁴, Fadi G. Alnaji⁵, Kelsie J. Green^{1,6}, Leyi Wang⁷, Richard L. Fredrickson⁷, Tong Wang⁸, George N. Wong⁸, Johnny Uelmen⁹, Sergei Maslov^{2,8,10}, Zachary J. Weiner⁸, Alexei V. Tkachenko¹¹, Hantao Zhang¹², Zhiru Liu¹³, Ahmed Ibrahim¹⁴, Sanjay J. Patel¹⁵, John M. Paul¹⁶, Nickolas P. Vance¹⁷, Joseph G. Gulick^{17,65}, Sandeep Puthanveetil Satheesan¹⁸, Isaac J. Galvan¹⁷, Andrew Miller¹⁵, Joseph Grohens¹⁹, Todd J. Nelson¹⁷, Mary P. Stevens¹⁷, P Mark Hennessy²⁰, Robert C. Parker Jr²¹, Edward Santos²², Charles Brackett²², Julie D. Steinman⁷, Melvin R. Fenner Jr²¹, Kirstin Dohrer⁷, Michael DeLorenzo²³, Laura Wilhelm-Barr²³, Brian R. Brauer²⁴, Catherine Best-Popescu¹⁰, Gary Durack^{16,25}, Nathan Wetter²⁵, David M. Kranz²⁶, Jessica Breitbarth⁶, Charlie Simpson⁶, Julie A. Pryde²⁷, Robin N. Kaler²⁸, Chris Harris²⁸, Allison C. Vance²⁸, Jodi L. Silotto²⁸, Mark Johnson⁶, Enrique Andres Valera^{10,16}, Patricia K. Anton²⁹, Lowa Mwilambwe³⁰, Stephen P. Bryan³¹, Deborah S. Stone³², Danita B. Young³⁰, Wanda E. Ward²³, John Lantz³¹, John A. Vozenilek¹⁶, Rashid Bashir¹⁶, Jeffrey S. Moore^{2,32}, Mayank Garg³², Julian C. Cooper³², Gillian Snyder³³, Michelle H. Lore³³, Dustin L. Yocum³⁴, Neal J. Cohen^{31,35}, Jan E. Novakofski³⁶, Melanie J. Loots³⁷, Randy L. Ballard³⁸, Mark Band³⁹, Kayla M. Banks⁶, Joseph D. Barnes⁴⁰, Iuliana Bentea⁴¹, Jessica Black⁴², Jeremy Busch³⁸, Abigail Conte⁴³, Madison Conte⁴⁴, Michael Curry⁴², Jennifer Eardley⁶, April Edwards⁷, Therese Eggett⁷, Judes Fleurimont⁴⁰, Delaney Foster⁴⁵, Bruce W. Fouke^{2,5,39}, Nicholas Gallagher⁴⁶, Nicole Gastala⁴³, Scott A. Genung⁴⁷, Declan Glueck⁴², Brittani Gray⁴⁰, Andrew Greta⁴⁸, Robert M. Healy⁶, Ashley Hetrick⁴⁹,

Arianna A. Holterman³¹, Nahed Ismail⁴¹, Ian Jasenof⁴⁰, Patrick Kelly⁴⁹, Aaron Kielbasa²³, Teresa Kiesel⁴⁹, Lorenzo M. Kindle¹⁷, Rhonda L. Lipking³⁹, Yukari C. Manabe ⁴⁴, Jade Mayes³⁸, Reubin McGuffin⁶, Kenton G. McHenry¹⁸, Agha Mirza⁴⁴, Jada Moseley⁴², Heba H. Mostafa⁴⁶, Melody Mumford⁴⁰, Kathleen Munoz⁴⁰, Arika D. Murray⁴², Moira Nolan⁵⁰, Nil A. Parikh³², Andrew Pekosz ^{43,44}, Janna Pflugmacher⁵¹, Janise M. Phillips²¹, Collin Pitts⁴⁹, Mark C. Potter⁵², James Quisenberry⁵³, Janelle Rear⁵⁴, Matthew L. Robinson⁴⁴, Edith Rosillo⁵⁵, Leslie N. Rye³⁹, MaryEllen Sherwood⁶, Anna Simon²³, Jamie M. Singson⁵³, Carly Skadden⁶, Tina H. Skelton³⁹, Charlie Smith⁷, Mary Stech²¹, Ryan Thomas⁴⁷, Matthew A. Tomaszewski⁵⁶, Erika A. Tyburski^{57,58}, Scott Vanwingerden⁵⁹, Evette Vlach⁷, Ronald S. Watkins^{48,60}, Karriem Watson⁴⁰, Karen C. White⁶, Timothy L. Killeen⁶¹, Robert J. Jones²³, Andreas C. Cangellaris⁶², Susan A. Martinis³⁷, Awais Vaid²⁷, Christopher B. Brooke ^{2,5}, Joseph T. Walsh ⁵⁵, Ahmed Elbanna ^{14,32}✉, William C. Sullivan ⁶³✉, Rebecca L. Smith ^{2,6,9,18}✉, Nigel Goldenfeld ^{2,8,64}✉, Timothy M. Fan ^{3,4}✉, Paul J. Hergenrother ^{1,2,3}✉ & Martin D. Burke ^{1,2,3,6,26,32}✉

¹Department of Chemistry, University of Illinois at Urbana-Champaign, Urbana, IL, USA. ²Carl R. Woese Institute for Genomic Biology, University of Illinois at Urbana-Champaign, Urbana, IL, USA. ³Cancer Center at Illinois, University of Illinois at Urbana-Champaign, Urbana, IL, USA. ⁴Department of Veterinary Clinical Medicine, University of Illinois at Urbana-Champaign, Urbana, IL, USA. ⁵Department of Microbiology, University of Illinois at Urbana-Champaign, Urbana, IL, USA. ⁶Carle Illinois College of Medicine, University of Illinois at Urbana-Champaign, Urbana, IL, USA. ⁷Veterinary Diagnostic Laboratory, University of Illinois at Urbana-Champaign, Urbana, IL, USA. ⁸Department of Physics, University of Illinois at Urbana-Champaign, Urbana, IL, USA. ⁹Department of Pathobiology, College of Veterinary Medicine, University of Illinois at Urbana-Champaign, Urbana, IL, USA. ¹⁰Department of Bioengineering, University of Illinois at Urbana-Champaign, Urbana, IL, USA. ¹¹Center for Functional Nanomaterials, Brookhaven National Laboratory, Upton, NY, USA. ¹²Computer Science, University of Illinois at Urbana-Champaign, Urbana, IL, USA. ¹³Department of Physics, Stanford University, Palo Alto, CA, USA. ¹⁴Department of Civil and Environmental Engineering, University of Illinois at Urbana-Champaign, Urbana, IL, USA. ¹⁵Department of Electrical and Computer Engineering, University of Illinois at Urbana-Champaign, Urbana, IL, USA. ¹⁶Grainger College of Engineering, University of Illinois Urbana-Champaign, Urbana, IL, USA. ¹⁷Technology Services, University of Illinois at Urbana-Champaign, Urbana, IL, USA. ¹⁸National Center for Supercomputing Applications, University of Illinois at Urbana-Champaign, Urbana, IL, USA. ¹⁹Department of English, University of Illinois at Urbana-Champaign, Urbana, IL, USA. ²⁰Inabyte, Navato, CA, USA. ²¹McKinley Health Center, University of Illinois at Urbana-Champaign, Urbana, IL, USA. ²²OSF Healthcare, Peoria, IL, USA. ²³Office of the Chancellor, University of Illinois at Urbana-Champaign, Urbana, IL, USA. ²⁴Illinois Fire Service Institute, Champaign, IL, USA. ²⁵Tekmill, Champaign, IL, USA. ²⁶Department of Biochemistry, University of Illinois at Urbana-Champaign, Urbana, IL, USA. ²⁷Champaign-Urbana Public Health District, Champaign, IL, USA. ²⁸Public Affairs, College of Media, University of Illinois at Urbana-Champaign, Urbana, IL, USA. ²⁹Housing Division, University of Illinois Urbana-Champaign, Urbana, IL, USA. ³⁰Office of the Vice Chancellor for Student Affairs, University of Illinois Urbana-Champaign, Urbana, IL, USA. ³¹Office of the Dean of Students, University of Illinois at Urbana-Champaign, Urbana, IL, USA. ³²Beckman Institute for Advanced Science and Technology, University of Illinois at Urbana-Champaign, Urbana, IL, USA. ³³Interdisciplinary Health Sciences Institute, University of Illinois at Urbana-Champaign, Urbana, IL, USA. ³⁴Office for the Protection of Human Subjects, University of Illinois at Urbana-Champaign, Urbana, IL, USA. ³⁵Department of Psychology, University of Illinois Urbana-Champaign, Urbana, IL, USA. ³⁶College of Agricultural, Consumer and Environmental Sciences, University of Illinois at Urbana-Champaign, Urbana, IL, USA. ³⁷Office of the Vice Chancellor for Research and Innovation, University of Illinois at Urbana-Champaign, Urbana, IL, USA. ³⁸Department of Intercollegiate Athletics, University of Illinois at Urbana-Champaign, Urbana, IL, USA. ³⁹Carver Biotechnology Center, University of Illinois at Urbana-Champaign, Urbana, IL, USA. ⁴⁰Mile Square Health Center, University of Illinois Health, Chicago, IL, USA. ⁴¹Department of Pathology, College of Medicine, University of Illinois at Chicago, Chicago, IL, USA. ⁴²Illinois Human Resources, University of Illinois Urbana-Champaign, Urbana, IL, USA. ⁴³W. Harry Feinstone Department of Molecular Microbiology and Immunology, Johns Hopkins Bloomberg School of Public Health, Baltimore, MD, USA. ⁴⁴Division of Infectious Diseases, Department of Medicine, Johns Hopkins School of Medicine, Baltimore, MD, USA. ⁴⁵Division of Campus Recreation, University of Illinois at Urbana-Champaign, Urbana, IL, USA. ⁴⁶Division of Medical Microbiology, Department of Pathology, Johns Hopkins University School of Medicine, Baltimore, MD, USA. ⁴⁷Office of the Chief Info Officer, University of Illinois at Urbana-Champaign, Urbana, IL, USA. ⁴⁸University of Illinois System Office, Urbana, IL, USA. ⁴⁹University Health Services, University of Wisconsin-Madison, Madison, WI, USA. ⁵⁰Office of Corporate Relations, University of Illinois at Urbana-Champaign, Urbana, IL, USA. ⁵¹University Administration, University of Illinois at Urbana-Champaign, Urbana, IL, USA. ⁵²Department of Family and Community Medicine, College of Medicine, University of Illinois at Chicago, Chicago, USA. ⁵³Division of Student Affairs, University of Illinois at Urbana-Champaign, Urbana, IL, USA. ⁵⁴Office of the Vice President for Economic Development and Innovation, University of Illinois System, Urbana, IL, USA. ⁵⁵Library Department, University of Illinois at Urbana-Champaign, Urbana, IL, USA. ⁵⁶Office of the Provost, University of Illinois at Urbana-Champaign, Urbana, IL, USA. ⁵⁷Atlanta Center for Microsystems Engineered Point-of-Care Technologies, Emory University School of Medicine, Children's Healthcare of Atlanta, and Georgia Institute of Technology, Atlanta, GA, USA. ⁵⁸Georgia Institute of Technology, Institute for Electronics and Nanotechnology, Atlanta, GA, USA. ⁵⁹IT Service Delivery, University of Illinois at Urbana-Champaign, Urbana, IL, USA. ⁶⁰Office of the President, University of Illinois System, Urbana, IL, USA. ⁶¹Gies College of Business, University of Illinois Urbana-Champaign, Urbana, IL, USA. ⁶²Office of the Provost, University of Illinois Urbana-Champaign, Urbana, IL, USA. ⁶³Department of Landscape Architecture, University of Illinois at Urbana-Champaign, Urbana, IL, USA. ⁶⁴Department of Physics, University of California San Diego, La Jolla, CA 92093, USA. ⁶⁵Deceased: Joseph G. Gulick. ✉email: elbanna2@illinois.edu; wcsulliv@illinois.edu; rldsvm@illinois.edu; nigelg@ucsd.edu; t-fan@illinois.edu; hergenro@illinois.edu; mdburke@illinois.edu